# Blood vessels restrain pancreas branching, differentiation and growth

Judith Magenheim[1], Ohad Ilovich[2], Alon Lazarus[1], Agnes Klochendler[1], Oren Ziv[1], Roni Werman[1], Ayat Hija[1], Ondine Cleaver[3], Eyal Mishani[2], Eli Keshet[1] and Yuval Dor[1,*]

## SUMMARY

How organ size and form are controlled during development is a major question in biology. Blood vessels have been shown to be essential for early development of the liver and pancreas, and are fundamental to normal and pathological tissue growth. Here, we report that, surprisingly, non-nutritional signals from blood vessels act to restrain pancreas growth. Elimination of endothelial cells increases the size of embryonic pancreatic buds. Conversely, VEGF-induced hypervascularization decreases pancreas size. The growth phenotype results from vascular restriction of pancreatic tip cell formation, lateral branching and differentiation of the pancreatic epithelium into endocrine and acinar cells. The effects are seen both in vivo and ex vivo, indicating a perfusion-independent mechanism. Thus, the vasculature controls pancreas morphogenesis and growth by reducing branching and differentiation of primitive epithelial cells.

KEY WORDS: Pancreas development, VEGF, Blood vessels, Branching, Organ size, Vascular niche, Mouse

## INTRODUCTION

The primary function of blood vessels is to provide organs with oxygen and nutrients that are essential for tissue growth and maintenance. In recent years, additional roles of vascular endothelial cells in organ development and tissue homeostasis have been discovered. In the case of the embryonic liver and pancreas, seminal studies have shown that blood vessels provide perfusion-independent paracrine signals, which are crucial for early stages of organ development and differentiation (Jacquemin et al., 2006; Lammert et al., 2001; Matsumoto et al., 2001; Yoshitomi and Zaret, 2004). Paracrine factors secreted from endothelial cells also support adult liver regeneration (LeCouter et al., 2003). Survival and proper function of adult pancreatic β-cells were shown to depend on extracellular matrix produced by blood vessels (Nikolova et al., 2006; Zaret, 2006). In addition, it has been proposed that a 'vascular niche' maintains self-renewal in several adult stem cell systems, including the brain, testis, bone marrow and fat (Butler et al., 2010b; Palmer et al., 2000; Shen et al., 2008; Tang et al., 2008; Tavazoie et al., 2008; Yoshida et al., 2007). At least for neuronal and hematopoietic stem cells, blood vessels are able to impact self-renewal in vitro in the absence of blood flow, demonstrating the importance of paracrine signals from endothelial cells (Butler et al., 2010b; Shen et al., 2004). The effects of blood vessels on self-renewal of hematopoietic stem cells appear to involve the activation of Notch signaling within stem cells (Butler et al., 2010b).

Notably, the net effect of blood vessels on tissue development in all these cases is seemingly a positive one. Endothelial cells provide important cues for early organ formation, maintain stem cell potential and help carrying the limiting nutrients needed for tissue growth beyond the minimal size afforded by passive diffusion.

Here, we describe a series of experiments that examine the role of blood vessels during the morphogenetic stages of pancreas development, using both endothelial cell ablation and forced hypervascularization. During these stages (embryonic days 10-13 in the mouse), the pancreas starts to undergo an extensive process of branching morphogenesis, growth and the beginning of differentiation (Cleaver and MacDonald, 2009; Gittes, 2009; Jorgensen et al., 2007; Murtaugh, 2007; Oliver-Krasinski and Stoffers, 2008). At the tip of each branch, rapidly dividing cells that express Cpa1 and Ptf1a are multipotent progenitors, which leave behind 'trunk' cells (Zhou et al., 2007). As shown by time-lapse studies (Cleaver and MacDonald, 2009; Puri and Hebrok, 2007; Solar et al., 2009) and lineage tracing (Solar et al., 2009), trunks can give rise to new lateral branches headed by tips. Endocrine progenitor cells expressing neurogenin 3 (Ngn3) emerge in the trunks, delaminate and differentiate to hormone-producing cells that will coalesce to form the islets of Langerhans. Trunk cells eventually form the differentiated ductal epithelium. Tip cells differentiate later in development to acinar cells, which secrete digestive enzymes to the ducts (Zhou et al., 2007). We show that in this context, perfusion-independent signals from blood vessels surprisingly act to slow down organ growth and have a net negative effect on organ size. The underlying mechanism is vascular sustenance of a simple tubular pancreatic epithelium, and the restriction of pancreas tip and endocrine progenitor cell formation. Consequently, blood vessels favor reduced branching and inhibit endocrine and exocrine differentiation.

## MATERIALS AND METHODS

### Mice

Pdx1-tTA mice (Holland et al., 2002) were the generous gift from Ray MacDonald (University of Texas Southwestern, TX, USA). TET-VEGF (Dor et al., 2001), TET-sFLT1 (Dor et al., 2001; May et al., 2008), Flk1-lacZ (Shalaby et al., 1997) and Pdx1-GFP (Gu et al., 2004) mice have been described previously. Embryos were genoyped by PCR using the following primers: Pdx1-tTA, 5′-TAGATGTGCTTTACTAAGTCATCGCG-3′ and

[1]Department of Developmental Biology and Cancer Research, The Institute for Medical Research Israel-Canada, The Hebrew University-Hadassah Medical School, Jerusalem 91120, Israel. [2]Cyclotron/Radiochemistry Unit, Hadassah-Hebrew University Medical Center, Jerusalem, 91120, Israel. [3]Department of Molecular Biology, UT Southwestern Medical Center, Dallas, TX 75235, USA.

*Author for correspondence (yuvald@ekmd.huji.ac.il)

5′-GAGATCGAGCGGGCCCTCGATGGTAG-3′; TET-VEGF, 5′-CGCGAAGCTTCCACCATGGACTTTCTGCTCTCTTGGGGT-3′ and 5′-CGCGGATATCACCGCCTTGGCTTGTCACA-3′; Flk1-lacZ, 5′-CAACAGTTGCGCAGCCTGAATGG-3′ and 5′-AAATCGCTGAT-TTGTGTAGTCGGT-3′; Pdx1-GFP, 5′-TCGTGGAACTGGATGG-CGATG-3′ and 5′-CTTCAGCTCGATTCTATTCACCA-3′. The joint ethics committee (IACUC) of the Hebrew University and Hadassah Medical Center approved the study protocol for animal welfare. The Hebrew University is an AAALAC International accredited institute.

## Pancreatic explants

Pancreatic buds were cultured on filters, in the liquid-air interface, as previously described (van Eyll et al., 2004). Briefly, the dorsal pancreatic bud from embryonic day (E)12.5 mouse embryos was excised under a dissecting microscope in Hank's balanced salts solution (HBSS). Alternatively, the gut and pancreas from E9.5 embryos were isolated. The explants were cultured in DMEM supplied with 10% fetal bovine serum, containing 100 U/ml penicillin and 100 μg/ml streptomycin. Explants were cultured on microporous membranes and no medium was added on top of the filter, so that the tissue grew at the air/medium interface. Medium was changed every other day.

To ablate endothelial cells in pancreatic explants, we used 1-[4-(6,7-Dimethoxy-quinolin-4-yloxy)-3-fluoro-phenyl]-3-(2-fluoro-phenyl)-urea (Ilovich et al., 2008) (VEGFR2i). The molecule has a low $IC_{50}$ (5-15 nM) to VEGFR2 and PDGFRb, and a high $IC_{50}$ (>500 nM) for IGF1R, EGFR and Her2. Drug was dissolved in DMSO (stock solution 25 mM) and added to explants at a final concentration of 100 nM. γ-Secretase inhibitor XX (Calbiochem, catalog number 565789), was added to explants at a final concentration of 100 nM.

## Immunostaining, antibodies and microscopy

Whole-mount immunostaining was performed essentially as described previously (Ahnfelt-Ronne et al., 2007b). Alternatively, staining was performed on 5 μm paraffin sections of dissected guts (E15.5) or isolated pancreata (E15.5-P3). Tissue was fixed in 4% buffered zinc-formalin for 2 hours at 4°C, dehydrated in an ethanol series, cleared in histoclear and embedded in Paraplast (Kendall). When required, antigen retrieval was performed using a pressure cooker. Primary antibodies used in this study included: guinea pig anti-insulin (1:500; DAKO), armenian hamster anti-Muc1 (1:250; Labvision), rat anti-CD31/Pecam (1:50; BD), rabbit anti-amylase (1:100; Sigma), rabbit anti-carboxypeptidase 1 (1:200; Rockland), guinea pig, goat and rabbit anti-Pdx1 (1:2500; a generous gift from Chris Wright, Vanderbilt University, TN, USA), rabbit anti-ptf1a (1:2000; Beta Cell Biology Consortium), rabbit anti-Ngn3 (1:500; Beta Cell Biology Consortium), guinea pig anti-Ngn3 (1:500; a generous gift from Maike Sander, UCSD, CA, USA), mouse anti-Nkx2.2 (1:50; Developmental Studies Hybridoma Bank), rabbit anti Nkx6.1 (1:800; Beta Cell Biology Consortium), rabbit anti phospho histone H3 (PHH3) (1:100; Cell Signaling), rabbit anti active caspase 3 (1:100; Cell Signaling), and Hypoxyprobe (Hypoxyprobe Kit, Chemicon). For DNA counterstain we used DAPI (Sigma). Secondary antibodies were from Jackson ImmunoResearch, used at 1:200. Immunofluorescence images were captured on a Nikon C1 confocal microscope or Olympus FV1000. For FACS analysis, E15.5 pancreata from Pdx1-GFP embryos were dissociated to single cells with Collagenase P (2 mg/ml, Roche), and stained with either Apc-conjugated anti-Flk1 (1:20; BD) or rabbit anti-Flt1 (1:100; Santa Cruz) followed by a secondary antibody Cy5 anti-rabbit (1:800; Jackson). To measure proliferation by FACS, E12.5 explants treated for 3 days with VEGFRi or vehicle were dissociated and stained with antibodies against Pdx1 and Ki67, followed by fluorophore-conjugated secondary antibodies.

## RNA

For RT-PCR, total RNA was prepared using Qiagen RNeasy microkit according to the manufacturer's protocol. Total RNA (100 ng) was used for first-strand cDNA synthesis using random primers (Roche) and reverse transcriptase (ImProm-II, Promega). Quantitative real-time PCR was performed with SYBR Green PCR master mix (Applied Biosystems) in 96-well plates using the 7900HT instrument (Applied Biosystems). All reactions were performed in triplicates. The relative amount of Ngn3

mRNA was calculated using the comparative CT method after normalization to Pdx1. Primer sequences were: Ngn3, 5′-ACTGACCTGCTGCTCTCTATTCTTT-3′ and ACTGACCTGC-TGCTCTCTATTCTTT-3′; Pdx1, 5′-AGGCCAGTGGGCAGGAG-3′ and 5′-CTCTTGTTTTCCTCGGGGTTCC-3′. For transcriptome analysis, RNA was isolated using QIAGEN RNeasy micro Kit from pancreatic buds of Pdx1-tTA (n=3) and littermate Pdx1-tTA; TET-VEGF (n=3) E12.5 embryos, or from E12.5 wild-type pancreatic buds explanted and treated with VEGFR2i (n=5) or vehicle (n=5) for 2 days. Affymetrix mouse gene 1.0 st arrays were used. The arrays were RMA normalized using Partek Genomic Suite 6.5. Differentially regulated genes were selected based on P-values and ratios using t-test. Data are deposited in Gene Expression Omnibus (Accession Number GSE32098).

## Analysis

To measure the area of explants stained in whole mount we obtained confocal z-stacks of the whole tissue. The fraction of tissue covered by Pdx1 or Muc1 staining was determined using NIS-Elements software. Significance was determined using two-tailed Student's t-test. A P-value less than 0.05 was considered significant. Data are presented as mean±s.e.m.

# RESULTS
## Blood vessels restrict the size of the developing pancreas

To examine the role of blood vessels in pancreas morphogenesis and growth, we manipulated the vasculature of the embryonic pancreas. To enhance the formation of blood vessels, we crossed Pdx1-tTA and TET-VEGF transgenic mice (Dor et al., 2001; Holland et al., 2002) to drive expression of vascular endothelial growth factor (VEGF) specifically in the pancreas. Importantly, VEGF receptors are not expressed in the pancreatic epithelium (see Fig. S1 in the supplementary material), indicating that any effect of VEGF on the epithelium will be indirect, via the vasculature. As expected, VEGF expression led to massive hypervascularization of the pancreas, evident by the intense staining for the endothelial cell marker Pecam (Fig. 1A). Surprisingly, the pancreas of VEGF-expressing mice was significantly smaller compared with littermate controls, during embryonic development (see Fig. S2 in the supplementary material) as well as immediately after birth (Fig. 1B,C). Organ size was assessed by documenting total organ size and weight (in newborns) or total Pdx1-stained area (in embryos). As the absolute mass of blood vessels in transgenic mice was increased, the smaller organ size represented an even more dramatic inhibition of growth of the parenchymal component of the pancreas.

To rule out a possible non-specific toxic effect of hypervascularization, we performed reciprocal loss of function experiments. Pancreata were isolated from E12.5 wild-type embryos and cultured on filters, in the liquid-gas interface (van Eyll et al., 2004). Explants were treated with a small molecule inhibitor of VEGFR2 (VEGFR2i) (Ilovich et al., 2008), which led to a rapid and total ablation of endothelial cells, seen as a complete loss of staining for Pecam (Fig. 1D). To validate that endothelial cells were eliminated and have not simply lost Pecam expression, we treated Flk1-LacZ explants with the same inhibitor. Loss of X-Gal staining confirmed that endothelial cells were indeed efficiently ablated (Fig. 1D). In agreement with the TET-VEGF experiments, elimination of endothelial cells led to a significant increase in organ size after 3 days of culture, evident from the larger area stained for the pancreatic marker Pdx1 relative to vehicle-treated explants (Fig. 1E,F). Vehicle and VEGFR2i-treated explants had similar heights, as determined by confocal slices along the z axis, indicating that avascular buds had a larger total volume (see Fig. S3 in the supplementary material). As
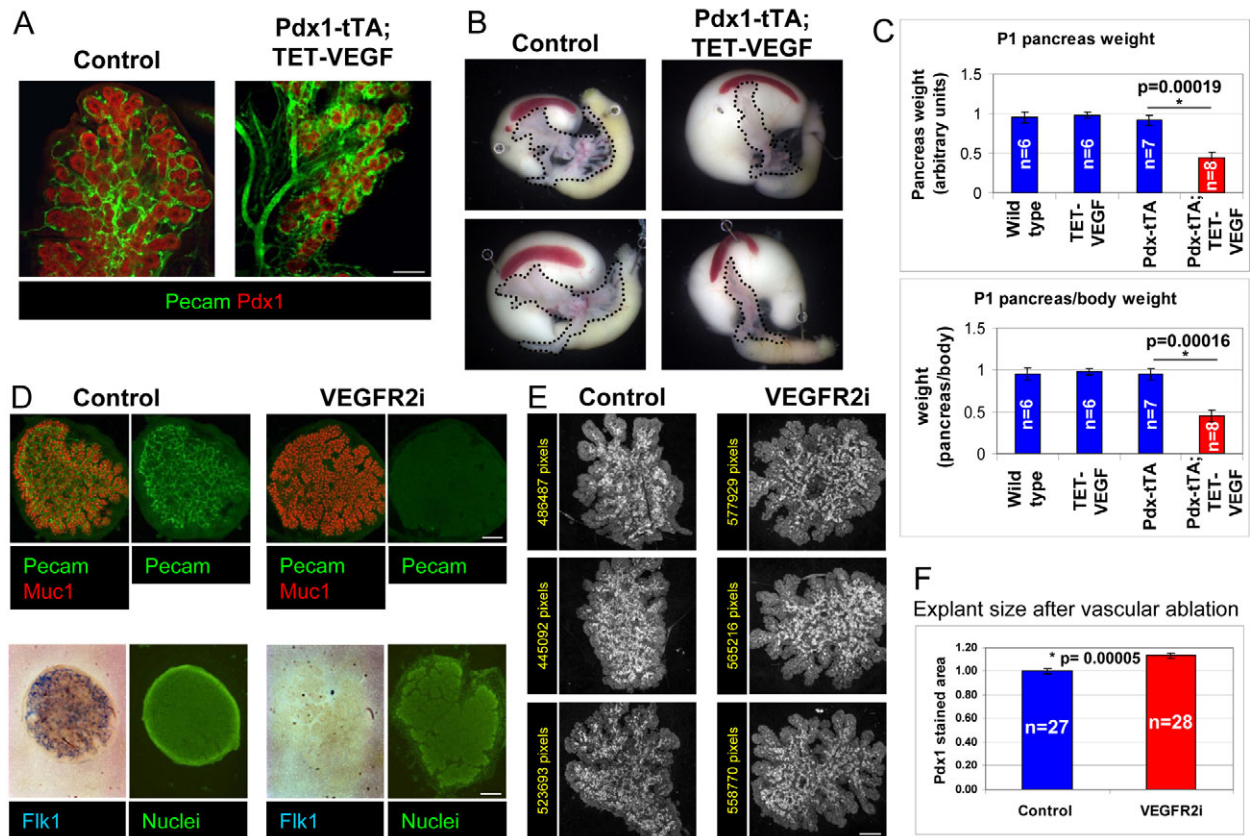
**Fig. 1. The vasculature restricts pancreas growth.** (**A**) Hypervascularization of pancreata overexpressing VEGF. Whole-mount staining for Pecam (green) and Pdx1 (red) in pancreata from an E13.5 Pdx1-tTA; TET-VEGF embryo and a control littermate. Scale bar: 100 μm. (**B**) Smaller pancreas in newborn mice (postnatal day 1) overexpressing VEGF. Dotted lines mark the pancreas. Among control animals, top image is from a Pdx1-tTA animal and bottom image is from a TET-VEGF animal. All images are from the same litter. (**C**) Reduced pancreas weight in newborn mice overexpressing VEGF. *n* describes the number of mice analyzed. Graphs show cumulative data from three litters. In each litter, wild-type pancreas weight was normalized to 1, to correct for inter-litter differences. Data are mean±s.e.m. (**D**) Elimination of endothelial cells upon treatment of pancreatic explants with VEGFR2 inhibitor. Pancreatic buds from E12.5 wild-type embryos were cultured for 3 days in the presence or absence of VEGFR2i. In the lower panels, mice contained a Flk1-*LacZ* reporter allele. X-gal stains blood vessels in such mice. Scale bars: 200 μm (top); 80 μm (bottom). (**E**) Larger size of E12.5 pancreatic buds cultured for 3 days in the presence of VEGFR2i. Images show confocal *z*-stacks of explants in whole-mount stained for Pdx1. Shown are representative images from three individual explants. Yellow numbers describe the area stained for Pdx1. Scale bar: 200 μm. (**F**) Quantification of explant size after treatment with VEGFR2i, as in E. *n* describes the total number of explants analyzed. Graphs show cumulative data from ten experiments using ten independent litters. Data are mean±s.e.m.

with the VEGF-expressing pancreas, the larger organ size in the face of reduced vasculature suggests that our measurements underestimate the impact on growth of the pancreas.

Finally, we took an independent genetic approach to eliminate blood vessels in the pancreas. Using the same Pdx1-tTA driver line described above, we overexpressed in the pancreatic epithelium a soluble receptor of VEGF, which acts as an efficient VEGF-trap (TET-sFLT1) (May et al., 2008). Expression of the sFLT1 transgene led to a dramatic reduction of blood vessel density in the developing pancreas (see Fig. S4 in the supplementary material). In vivo, this led to tissue hypoxia beyond embryonic day 11.5, followed by massive apoptosis, failure of pancreas development and death of newborn mice (see Fig. S4 in the supplementary material). The likely contribution of hypoxic stress to this phenotype precluded the analysis of Pdx1-tTA; TET-sFLT1 mice in vivo. However, explant cultures of E9.5 pancreatic buds from Pdx1-tTA; TET-sFLT1 mice grew to a size significantly larger than control littermates (see Fig. S5 in the supplementary material), consistent with the results obtained using the pharmacological inhibitor of VEGFR2.

Taken together, these results reveal that, contrary to expectation, blood vessels restrict the growth of the embryonic pancreas. The function of blood vessels is perfusion independent, as the same effects are seen in vivo and in explants, cultured in ambient oxygen and standard culture medium in the absence of blood flow.

## Reduced branching and differentiation in hypervascularized pancreata

To study the basis for the surprising negative effect of blood vessels on pancreas size, we examined how the patterns of branching morphogenesis and differentiation are affected by VEGF overexpression. Examination of VEGF-expressing pancreata revealed a striking block in branching at E12.5, apparent from immunostaining for either Muc1 (Fig. 2A) or Pdx1 (Fig. 2B and see Fig. S6 in the supplementary material). Transgenic pancreata had fewer branches, and instead presented with elongated unbranched tubes.

To determine whether multi-potent tip cells were affected by VEGF overexpression, we examined the expression pattern of the tip cell marker Cpa1. As shown in Fig. 2B, transgenic pancreata had a
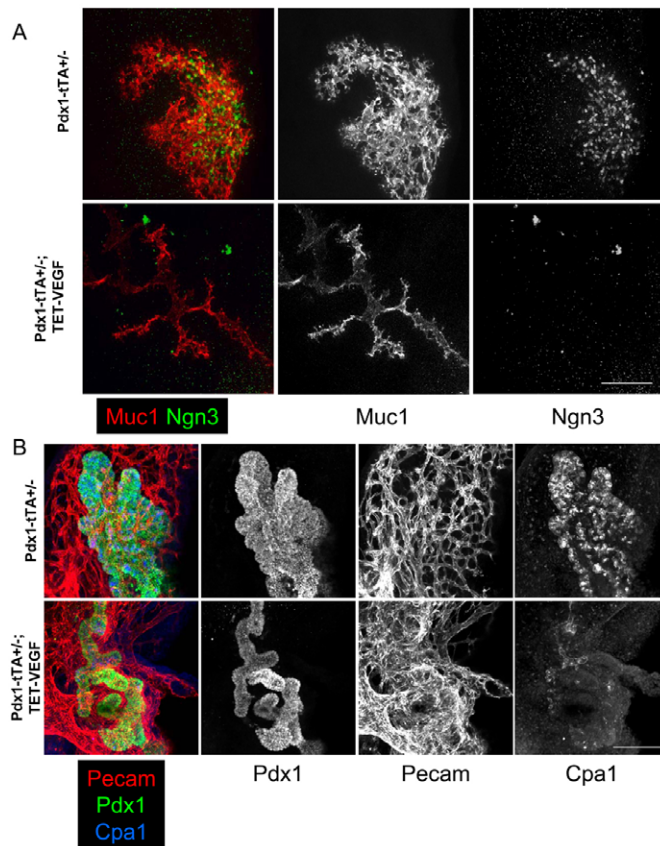
**Fig. 2. Reduced branching, tip cell formation and endocrine specification in pancreata from E12.5 embryos overexpressing VEGF.** (**A**) Whole-mount immunostaining for Muc1 (red) and Ngn3 (green), showing reduced branching and fewer Ngn3+ cells in VEGF-expressing pancreata. (**B**) Whole-mount immunostaining for Pdx1 (green), Pecam (red) and Cpa1 (blue), showing elongated unbranched tubes and fewer tip cells in VEGF-expressing pancreata. Scale bars: 200 μm. Images are z-stacks of serial confocal sections.

dramatic reduction in Cpa1 staining. Similar results were obtained with another tip marker, the transcription factor Ptf1a (see Fig. S6 in the supplementary material). Both Cpa1 and Ptf1a are also expressed in differentiated acinar cells, and thus changes in their expression could reflect a delay in acinar cell differentiation, rather than a change in tip cell formation. To examine this possibility, we stained embryonic pancreata for the definitive acinar cell marker amylase, which is absent from multipotent tip cells. Amylase expression was absent in E12.5 pancreata (see Fig. S7 in the supplementary material), consistent with Cpa1 and Ptf1a expression marking multipotent tip cells, rather than differentiated acinar cells. Thus, hypervascularization blocks tip cell formation and branching.

We then examined endocrine lineage development in transgenic embryos. Strikingly, expression of the key marker of endocrine progenitor cells, Ngn3, was nearly abolished in E12.5 VEGF-expressing pancreata (Fig. 2A). This suggests that blood vessels inhibit the development of both exocrine and endocrine lineages in the pancreas.

Finally, we characterized the unbranched tubes in Pdx1-tTA; TET-VEGF pancreata. Epithelial cells in E13.5 transgenic pancreata expressed key markers of undifferentiated trunk epithelium (Cleaver and MacDonald, 2009; Zhou et al., 2007), including Pdx1 (Fig. 2B), Nkx2.2 and Nkx6.1 (see Fig. S8 in the

supplementary material). These results suggest that hypervascularization does not induce duct differentiation, but rather supports the maintenance of trunk tubular epithelium.

To validate the immunofluorescence results at the mRNA level, we harvested pancreata from E12.5 VEGF-overexpressing embryos and control littermates, prepared RNA and compared their transcriptomes using Affymetrix microarrays. The analysis of transcriptome data confirmed the finding that VEGF overexpression led to a dramatic increase in the number of vascular endothelial cells, and a concomitant decrease in the level of endocrine progenitor cells, as well as their differentiation products. Interestingly, although markers of differentiated acinar cells are not detected at this age at the protein level in wild-type embryos, mRNA for acinar genes is already expressed at significant levels. Similar to its impact on differentiated endocrine cell markers, VEGF overexpression led to a decrease in the level of acinar cell markers such as Amylase and elastase (see Fig. S9, Table S1 and Table S2 in the supplementary material).

Together, these results show that VEGF-driven hypervascularization reduces the formation of multipotent tip cells, reduces branching, and prevents endocrine and exocrine differentiation of the embryonic pancreas, while sustaining primitive undifferentiated (proto-differentiated) epithelial cells. These combined effects can account for the unexpected smaller size of transgenic pancreata shown above.

## The effects of VEGF on branching and differentiation are perfusion independent
To determine whether the effects of VEGF and hypervascularization on pancreas branching and differentiation depend on blood flow, we isolated pancreatic buds from VEGF-expressing embryos and cultured them on filters in complete medium and ambient oxygen. As shown in Fig. 3A, transgenic E10.5 buds explanted for 3 days were smaller compared with wild-type littermates, had an altered pattern of Muc1 staining, indicative of defective branching, and had only faint staining for Ngn3. Similarly, VEGF-expressing E12.5 buds explanted for 2 days had a dramatic reduction in size and branching compared with control littermates (Fig. 3B). In addition, transgenic explants had fewer Ngn3+ cells and fewer insulin+ cells, showing that the reduction of endocrine progenitor cells results in fewer downstream differentiation products.

To control for potential early effects of VEGF expression in vivo, we treated pregnant females with tetracycline to repress transgenic VEGF expression until the time of culture at E10.5. Transgenic embryos at E10.5 were indistinguishable from wild-type littermates (Pecam, Pdx1 and Ngn3 expression patterns), suggesting efficient repression of the VEGF transgene. However, after 3 days of culture in the absence of tetracycline, VEGF-expressing explants had more blood vessels (not shown) and a dramatic decrease in Ngn3+ cells (see Fig. S10 in the supplementary material).

These results show that the repressive effect of blood vessels on pancreas branching and endocrine differentiation is not mediated through blood flow, circulating cells or plasma factors, nutrients or oxygen. Rather, factor(s) produced by vascular endothelial cells are likely to be responsible for this effect.

## Ablation of endothelial cells triggers tip cell formation and differentiation
The experiments with transgenic mice overexpressing VEGF suggest a novel role for blood vessels in restraining branching and differentiation. We therefore used our loss-of-function
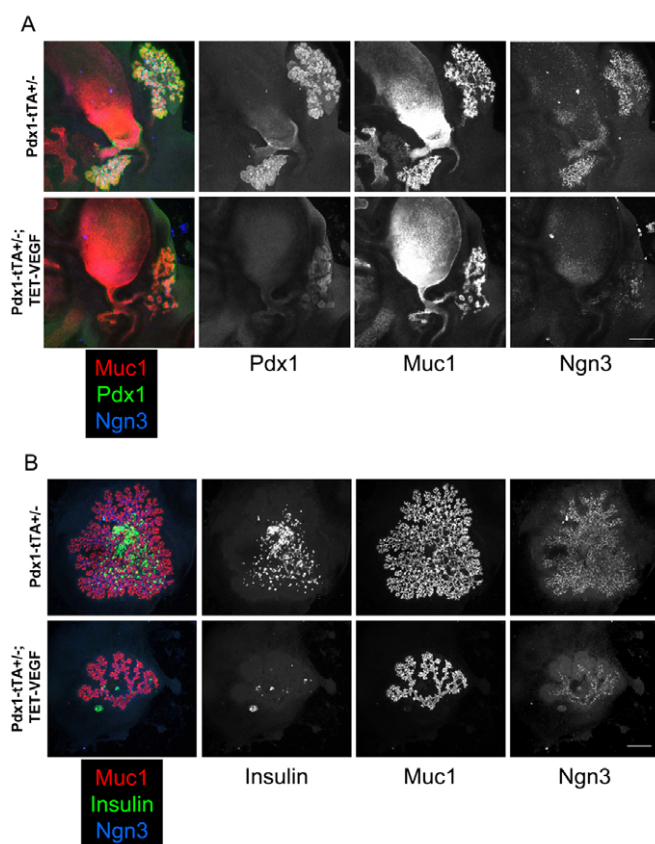
**Fig. 3. Reduced branching and endocrine differentiation in explanted Pdx1-tTA; TET-VEGF pancreatic buds, suggesting perfusion-independent effects of hypervascularization.**
(**A**) Whole-mount immunostaining for Pdx1 (green), Muc1 (red) and Ngn3 (blue) in E10.5 buds cultured for 3 days. (**B**) Whole-mount immunostaining for insulin (green), Muc1 (red) and Ngn3 (blue) in E12.5 buds cultured for 2 days. Note smaller size, reduced branching and reduced numbers of β-cells in VEGF-expressing pancreata. Scale bars: 200 μm.

approach to examine whether the endogenous vasculature has similar effects during pancreas development. E12.5 pancreatic explants from wild-type mice were cultured for 2-3 days in the presence of VEGFR2i, which totally ablated vascular endothelial cells as shown in Fig. 1D. We then compared branching and differentiation in VEGFR2i-treated and control explants, using whole-mount immunostaining. We used the pattern of Muc1 staining as a convenient readout for tips and trunks. In normal explants, tips located in the periphery show strong and dense staining for Muc1, overlapping with established tip markers such as Cpa1 and Ptf1a, whereas large trunks in central areas stain more weakly for Muc1 (see Fig. S11 in the supplementary material). In further support of the use of Muc1 pattern as a tip/trunk indicator, the key trunk marker Hnf1β colocalized with weakly stained Muc1, whereas the dense clusters strongly expressing Muc1 were largely Hnf1β negative (see Fig. S12 in the supplementary material). VEGFR2i treatment eliminated the center/periphery dichotomy in Muc1 staining, and essentially transformed the whole explant into a homogenous field exhibiting a peripheral pattern of Muc1 staining (Fig. 4A). A similar trend was seen in the pattern of the tip cell marker Ptf1a. Although in control explants cultured for 2 days Ptf1a was

expressed in discrete foci, vascular ablation caused a more extensive and uniform distribution of Ptf1a protein, consistent with widespread formation of tips in central areas of the bud (Fig. 4B).

Tip cells eventually give rise to acinar cells. To examine whether endothelial cell ablation triggered acinar differentiation, we stained explants for amylase. In E12.5 buds cultured for 3 days, amylase^{+} cells appear mostly in the periphery, reflecting the location of tip cells. By contrast, in VEGFR2i-treated explants the domain of amylase expression expanded into central areas of the bud, normally containing mostly trunks (Fig. 4C). Quantification of amylase staining intensity relative to Pdx1 staining showed a significant, >2 fold, increase in the amylase-stained area (Fig. 4C). Consistent with this finding, western blotting revealed a striking 2.2-fold increase in the amount of amylase protein in explants that were exposed to VEGFR2i, when normalized to β-actin (Fig. 4D). In agreement with these data, expression of the tip/acinar marker Cpa1 expanded beyond peripheral tips, to abundant expression in central areas in VEGFRi-treated explants (see Fig. S13 in the supplementary material). Last, the mRNA levels of multiple acinar genes were significantly increased upon vascular ablation (Fig. 4E).

We then asked whether the formation of endocrine progenitor cells was also affected by ablation of blood vessels. Wild-type buds were cultured in the presence or absence of VEGFR2i, and stained in whole mount for endocrine progenitor cells. In cultures of E12.5 buds, vascular ablation had no detectable effect on endocrine progenitor cells (not shown). However, E9.5 explants cultured for 6 days in the presence of VEGFR2i had more Ngn3^{+} cells (Fig. 5A). To validate and quantify these results, we extracted RNA from remaining explants of the same litter, and determined the levels of Ngn3 mRNA using quantitative RT-PCR. In agreement with immunostaining results, avascular explants had a significant increase in Ngn3 mRNA (Fig. 5B). Thus, blood vessels restrain the formation of Ngn3^{+} endocrine progenitor cells during normal development of the pancreas.

Finally, we used microarray analysis to identify transcriptome changes in pancreatic explants upon vascular ablation. As expected, E12.5 explants treated with VEGFR2i for 2 days showed a dramatic reduction in the expression of vascular endothelial cell markers, reflecting efficient ablation of blood vessels (see Fig. S9, Table S3 and Table S4 in the supplementary material). Although endocrine cell markers showed little or no change in these samples, acinar cell markers such as amylase, elastase and Rnase1 were significantly upregulated compared with control explants (see Fig. S9 in the supplementary material), consistent with the western blot and immunofluorescence data. In summary, these results show that ablation of vascular endothelial cells induces the formation of tip cells and acinar differentiation, as well as the formation of endocrine progenitor cells.

## Evidence for involvement of Notch pathway in endothelial to epithelial signaling

What is the molecular nature of the endothelial signals that restrain epithelial branching and differentiation? Delta-Notch signaling represents an attractive candidate for a mediator of this tissue interaction. Notch is a well-recognized regulator of pancreas differentiation decisions, acting to restrict Ngn3 cell formation and acinar cell differentiation; in fact, the phenotype of pancreata expressing a constitutively active Notch transgene is reminiscent of VEGF-expressing pancreata, in that endocrine and exocrine differentiation is inhibited (Hald et al., 2003; Murtaugh et al.,
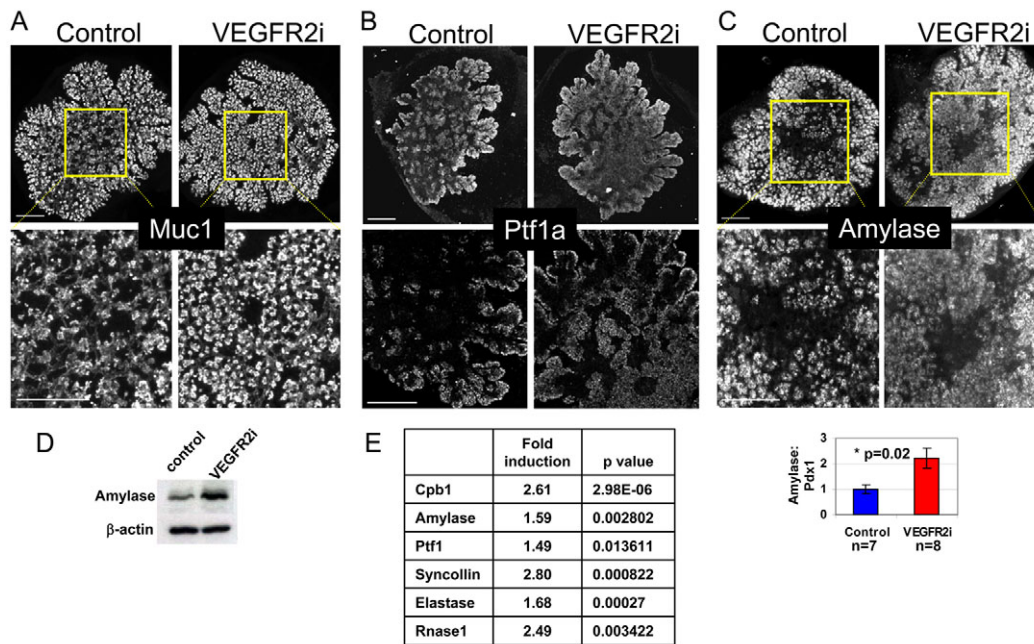
**Fig. 4. Excessive formation of tips and acinar differentiation upon ablation of endothelial cells in explanted pancreatic buds.** E12.5 wild-type buds were cultured with or without VEGFR2i and stained in whole mount. (**A**) Staining for Muc1 after culturing for 3 days. (**B**) Staining for Ptf1a after culturing for 2 days. Upper panels, *z*-stacks of 11 confocal sections. Bottom panels, individual confocal sections. (**C**) Top: staining for amylase after culturing for 3 days. Bottom: quantification of amylase-stained area in explants, normalized to the Pdx1-stained area. n denotes the number of individual explants analyzed. Data are mean±s.e.m. Bottom panels in A and C show higher magnification images of the areas marked in yellow in the upper panels. Scale bars: 200 μm. (**D**) Western blot showing increased amylase expression in avascular buds cultured as in C. Each lane represents a pool of three explants. The intensity of the amylase band relative to β-actin was increased 2.2-fold in the avascular samples. (**E**) Fold change in the mRNA levels of selected acinar cells upon vascular ablation. Data are extracted from microarray data (see Tables S1-4 and Fig. S9 in the supplementary material).

2003). Furthermore, Notch signaling has been recently implicated in vascular control of stem cell dynamics in neuronal (Shen et al., 2004) and hematopoietic stem cells (Butler et al., 2010b). We thus hypothesized that blood vessels affect branching and differentiation by modulating Notch signaling in the epithelium, either directly or via a relay (Jacquemin et al., 2006). To begin and examine this hypothesis, we treated hypervascular pancreatic explants with a pharmacological γ-secretase inhibitor (GSI), which prevents the activation of Notch. As shown in Fig. 6, GSI partially rescued the defects in Ngn3 cell formation and branching in VEGF-expressing explants. GSI induced the rapid expression of Ngn3 in the majority of epithelial cells in VEGF transgenics (Fig. 6), as well as in wild-type explants (Magenheim et al., 2011). Longer exposure to GSI caused thinning of tubes and excessive tip formation in both VEGF transgenics (Fig. 6) and wild-type explants (Magenheim et al., 2011). Therefore, the epithelium in hypervascularized pancreatic buds remains sensitive to Notch inhibition, supporting the idea that the vasculature could be acting by modulating an upstream step in epithelial Notch signaling. These results are consistent with the hypothesis that the vasculature restrains pancreas differentiation and branching at least in part via modulation of Notch signaling within the epithelium.

## DISCUSSION
### Vascular control of pancreas branching and differentiation
We show here that during pancreas development, blood vessels restrain pancreas tip cell formation and branching morphogenesis, and antagonize differentiation of epithelial cells into exocrine and endocrine fates. Consequently, the surprising net effect of blood vessels on pancreas development is inhibition of growth and a restriction of final organ size. The signals that mediate this response are independent of blood flow, circulating plasma factors and the provision of nutrients and oxygen, as manipulations of the vasculature lead to similar effects in vivo and in explants cultured in complete medium and ambient oxygen.

These findings seem counterintuitive and run against the well-established notion that blood vessels are positive regulators of tissue growth during development and postnatal life, as well as in pathologies such as cancer. How can our results be reconciled with this view? More specifically, how do our findings fit into the current understanding of pancreas development and morphogenesis, in particular the 'tip-trunk' model describing branching, progenitor cell dynamics and differentiation (Zhou et al., 2007)? We propose that epithelial cells in the developing pancreas, most of which reside in the trunks, face a fundamental choice. They can either divide symmetrically to generate two identical daughters, or take the differentiation/morphogenesis path, involving either the generation of a new, rapidly dividing tip cell followed by formation of a lateral branch (Puri and Hebrok, 2007; Solar et al., 2009), or the expression of Ngn3, followed by delamination and endocrine differentiation (Ahnfelt-Ronne et al., 2007a; Apelqvist et al., 1999).

Taking the first path, which we propose represents 'self-renewal', the epithelium generates elongated, unbranched tubes and retains multipotentiality. Taking the second path, the epithelium generates the branched pancreas, including its typical differentiated cell types. Proper development of the pancreas (and indeed, any
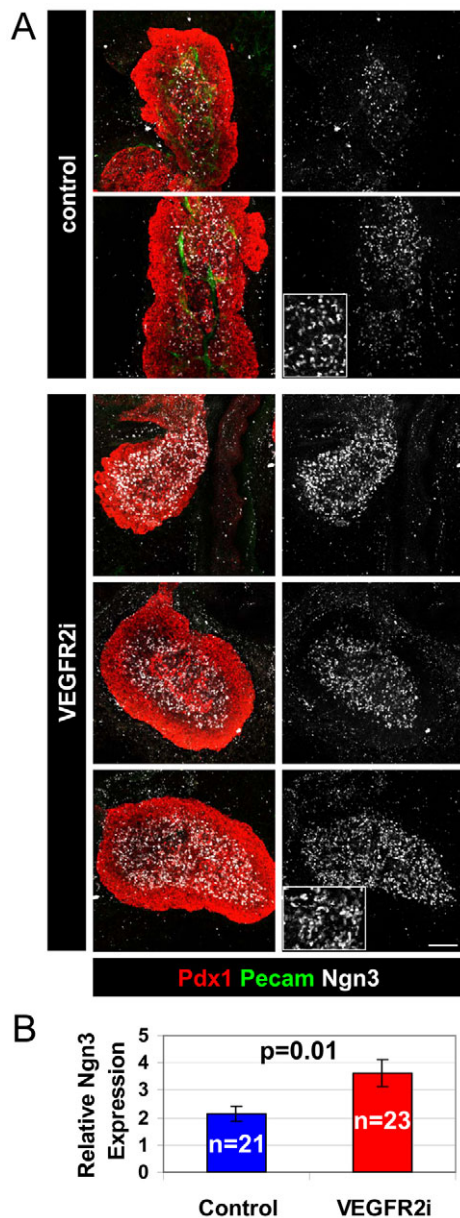
**Fig. 5. Accelerated formation of endocrine progenitor cells in avascular buds.** E9.5 wild type pancreatic buds were cultured for 6 days in the presence or absence of VEGFR2i. (**A**) Whole-mount immunostaining for Pdx1 (red), Pecam (green) and Ngn3 (white). Each image is a z-stack of one whole individual pancreas. Insets show a higher magnification of Ngn3-stained cells. Scale bar: 100 μm. (**B**) qRT-PCR for Ngn3, normalized to Pdx1 expression. Results shown are the combined data from six independent litters. n represents the total number of buds in each group. Data are mean±s.e.m.



**Fig. 6. Evidence for involvement of Notch pathway in endothelial signaling to the epithelium.** A γ-secretase inhibitor (GSI) partially rescues the branching and endocrine differentiation defects of Pdx1-tTA; TET-VEGF explants. GSI was added to E12.5 transgenic explants for 15 or 24 hours to document the patterns of Ngn3 and Muc1, respectively. Scale bars: 100 μm.

organ) must balance these two processes. In the absence of self-renewal, premature differentiation will deplete pools of stem/progenitor cells and compromise organ size and regenerative capacity, whereas a self-renewal bias will prevent branching and differentiation. We thus hypothesize that blood vessels are key regulators of the balance between self-renewal and branching/differentiation decisions of the pancreatic tubular trunk epithelium (see model, Fig. 7). In support of this hypothesis, we found that epithelial cells in hypervascularized pancreata expressed markers of undifferentiated trunk epithelium such as Pdx1, Nkx2.2

and Nkx6.1, strongly suggesting that they did not become differentiated duct cells. Furthermore, VEGF-affected pancreatic epithelial cells retained their differentiation potential, as evidenced by the expression of Ngn3 and the normalization of branching pattern later in development, when transgenic VEGF expression was decreased (owing to reduced expression of Pdx1-tTA in the epithelium) (see Fig. S14 in the supplementary material). This was accompanied by perinatal loss of Nkx6.1 in the ductal epithelium and normal expression pattern of the duct marker cytokeratin 19 (see Fig. S8 in the supplementary material), consistent with normal duct differentiation. Nonetheless, the temporary block in branching during a crucial developmental stage was sufficient to reduce newborn organ size.

This view is consistent with recent reports on vascular niches acting to maintain adult stem cells in a self-renewing state. Such niches were shown for neuronal stem cells (Shen et al., 2008; Tavazoie et al., 2008), for spermatogonial stem cells (Yoshida et al., 2007), for hematopoietic stem cells (Butler et al., 2010b) and, potentially, for adipocyte progenitor cells (Tang et al., 2008). In the context of pancreas development, our results are consistent with a recent report that endothelial cells limit acinar differentiation, but with minimal impact on endocrine cells (Pierreux et al., 2010). This paper used either mosaic deletion of VEGF or the addition of recombinant VEGF to explants. We believe that the stronger impact on the vasculature afforded by our tools (complete elimination of endothelial cells by sFLT1 or VEGFRi, and transgenic overexpression of VEGF) exposed additional key effects of blood vessels on the developing pancreas. Thus, our study reveals that endothelial cells restrict not only exocrine differentiation, but also the formation of endocrine progenitor cells. In addition, we show that endothelial cells have a surprisingly

DEVELOPMENT
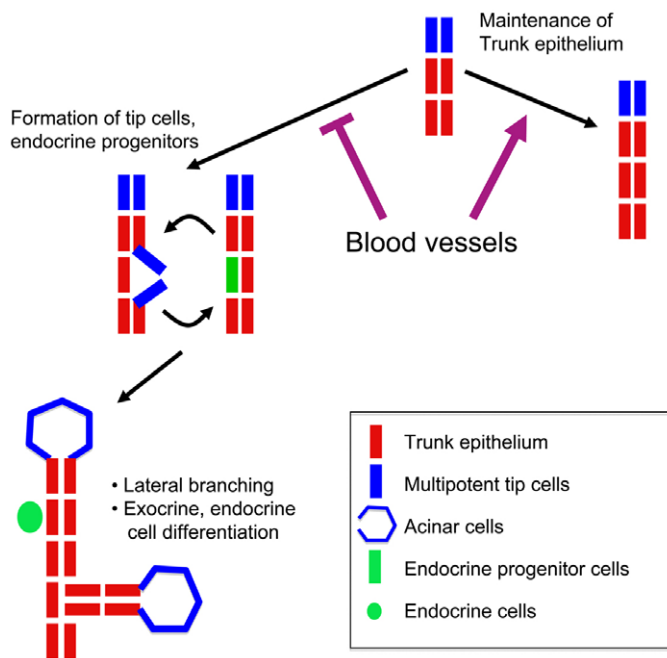
**Fig. 7. Model.** Perfusion-independent signals from blood vessels favor self-renewal of trunk pancreatic epithelium. This comes at the expense of forming Ngn3^{+} endocrine progenitors and multipotent tip cells. Consequently, blood vessels restrain the formation of lateral branches, acinar and endocrine differentiation. The net result is a paradoxical restriction of organ size by endothelial cells. We propose that the vasculature acts by modulating Notch-mediated lateral signaling in the epithelium, which favors the coupled formation of endocrine progenitors and tip cells. See text for details.

negative effect on organ size, and propose a general mechanism for the activity of the vascular niche in controlling pancreas differentiation, morphogenesis and growth.

We thus propose that a conserved function of endothelial cells is maintenance of progenitor pools. In the context of late pancreas development (but not in earlier stages prior to branching, see below), the net effect of vasculature-driven excessive self-renewal and deficient branching/differentiation is a smaller organ size. The surprising conclusion that blood vessels restrict organ size is consistent with a recent paper (Sand et al., 2011), which used S1P1 deficiency and vascular ablation in mice to show that endothelial cell hyperplasia negatively influences growth of the pancreas, stomach and liver.

It will be interesting to test whether signals from endothelial cells act in a similar manner in the context of adult tissue regeneration and tumorigenesis (Butler et al., 2010a). Progress in this direction may offer new insights into the role of the vasculature in regenerative biology, and into the mode of action of anti-angiogenic cancer therapy.

We note that an important aspect of the vascular effect on pancreas size remains unresolved. Differences in size could result from differences in cell number, cell size or the extracellular space. We could not find significant differences in the rate of cell proliferation and apoptosis between the epithelium of VEGF-expressing mice and control littermates, and between the epithelium of VEGFRi-treated and vehicle-treated explants (see Fig. S15 in the supplementary material). However, we believe that small differences in replication and apoptosis could be missed by

this analysis and still have a significant effect. We also examined the possibility that differences in organ size were the result of changes in the proportion of acinar cells, which are known to be much larger than other cell types in the adult pancreas. However, amylase^{+} cells in embryonic explants were not larger than adjacent amylase[–]; Pdx1^{–} cells, in both control and VEGFRi-treated explants (see Fig. S16 in the supplementary material). This result argues against the possibility that differences in cell size account for the differences in organ size upon vascular manipulations.

It is important to acknowledge a limitation of our experiments. Since all our manipulations targeted VEGF signaling, it is theoretically possible that the effect on pancreas development was mediated through a non-endothelial VEGFR+ compartment, and that the effect on the vasculature was an epiphenomenon. To address this possibility, we showed that VEGF receptors are not expressed in pancreatic epithelial cells, suggesting that VEGF cannot act directly on the epithelium. However it is more difficult to exclude the possibility that VEGF affects pancreas development via a non-endothelial, non-epithelial VEGFR+ compartment such as macrophages. While we could not rule out this formal possibility, we believe it is unlikely given the bulk of accumulated knowledge on the biology of vascular niches in multiple tissues.

### Early and late effects of blood vessels on pancreas development

Although our results appear at odds with previous studies which identified an essential role of blood vessels in pancreas development (Lammert et al., 2001; Yoshitomi and Zaret, 2004), we note that these studies addressed an earlier developmental stage, after organ specification but before the onset of branching morphogenesis and differentiation. It is possible that either endothelial cells produce different signaling molecules at different developmental stages, or alternatively, that molecular responses of the epithelium to the same signals change as development proceeds, as recently suggested (Zaret and Grompe, 2008). We favor a third alternative, whereby the same endothelial signals and the same signaling responses have different consequences at the tissue level depending on context.

During early stages of pancreas formation, self-renewing divisions are essential to generate a pool of stem/progenitor cells from which branches and differentiated products will emerge; interfering with this process by vascular ablation leads to a premature exhaustion of this pool and developmental failure, as reported before (Lammert et al., 2001; Yoshitomi and Zaret, 2004). During later stages of development, cell choices must gradually shift to branching (including the formation of rapidly dividing tip cells) and differentiation; in this setting, ablation of blood vessels will accelerate organ growth (if hypoxic effects are avoided, as in explants), and hypervascularization will restrain branching, differentiation and growth, as we observe. More experiments will be required to distinguish between these possibilities.

### Involvement of Notch signaling in vascular restriction of branching and differentiation

The molecular mechanism underlying the perfusion-independent interaction of blood vessels with the developing pancreas during early stages remains unknown to date (Jacquemin et al., 2006; Lammert et al., 2001; Yoshitomi and Zaret, 2004). As a first step towards identifying the molecular basis for the later endothelial-epithelial interaction that we report here, we considered Notch signaling. Of the central signaling pathways known to be involved in pancreas development, the Notch system represents a

particularly attractive candidate for mediating the effects of the vasculature on self-renewal versus differentiation (Esni et al., 2004; Hald et al., 2003; Murtaugh et al., 2003). The effects of forced Notch activation closely resemble the phenotype of VEGF overexpression, namely inhibition of endocrine differentiation and branching (Murtaugh et al., 2003). Moreover, Notch signaling within vascular niches has been implicated in the control of neuronal and hematopoietic stem cells (Butler et al., 2010b; Shen et al., 2004).

We found that pharmacological inhibition of intracellular Notch activation can partially rescue the VEGF phenotype, with regard to both endocrine differentiation and branching. Thus, the epithelium in VEGF-expressing pancreata remain sensitive to Notch inhibition, suggesting that blood vessels affect an upstream step in Notch signaling in the epithelium. This view is consistent with the recent report of Pierreux et al. that blood vessels positively regulate the Notch target genes *Hey1* and *Hey2* (Pierreux et al., 2010).

In light of these findings, we propose the following model (Fig. 7). Within the pancreatic epithelium, Notch-mediated lateral interactions cause the coupled formation of endocrine progenitor cells (cells downregulating Notch) and tip cells (adjacent cells upregulating Notch). We hypothesize that, normally, signals from blood vessels restrain these lateral interactions, perhaps by providing a constant low level of an endothelial Notch ligand (e.g. Dll4) that dampens the tendency of adjacent epithelial cells to undergo lateral inhibition, either losing or gaining Notch signaling. When blood vessels are eliminated, lateral interactions are uninhibited and lead to premature divergence of adjacent epithelial cells into low notch (endocrine) and high notch (tips). Hypervascularization prevents the Notch-controlled lateral divergence to endocrine/tip cells, and maintains the epithelium in a primitive proliferative state that might be termed 'self-renewal'. Genetic and gene expression studies are ongoing to test this model. Finally, it is entirely possible that additional signaling pathways affect the endothelial-epithelial interaction reported here. For example, endothelial cells could signal via the extracellular matrix and integrins (Kesavan et al., 2009; Nikolova et al., 2006) or via Fgf receptors (Hart et al., 2003; Jacquemin et al., 2006; Norgaard et al., 2003). More studies will be needed to test these ideas.

## Implications for directed differentiation of embryonic stem cells to beta cells

These findings may have practical implications for the derivation of transplantable, insulin-producing β-cells from embryonic stem cells (ESC) (D'Amour et al., 2006; Kroon et al., 2008). Our data may explain the failure of early attempts to use co-cultures of ESC and vascular endothelial cells for the derivation of β-cells (O.C., unpublished). It is becoming increasingly evident that the contribution of endothelial cell signals to pancreas and β-cell development is much more dynamic than previously assumed, and its practical use will have to take this complexity into account. Specifically, we propose that endothelial cells may positively influence the expansion of ESC-derived, multipotent pancreatic progenitor cells, but final differentiation may require the timed removal of endothelial cells at distinct intervals.

In summary, we show that blood vessels act to restrain pancreas branching and differentiation, leading to an overall restriction of organ growth. We propose that these effects reflect a conserved, perfusion-independent function of vascular endothelial cells, acting to favor self-renewal at the expense of branching and differentiation.

## Supplementary material
Supplementary material for this article is available at
http://dev.biologists.org/lookup/suppl/doi:10.1242/dev.066548/-/DC1

## References
**Ahnfelt-Ronne, J., Hald, J., Bodker, A., Yassin, H., Serup, P. and Hecksher-Sorensen, J.** (2007a). Preservation of proliferating pancreatic progenitor cells by Delta-Notch signaling in the embryonic chicken pancreas. *BMC Dev. Biol.* **7**, 63.

**Ahnfelt-Rønne, J., Jørgensen, M. C., Hald, J., Madsen, O. D., Serup, P. and Hecksher-Sørensen, J.** (2007b). An improved method for three-dimensional reconstruction of protein expression patterns in intact mouse and chicken embryos and organs. *J. Histochem. Cytochem.* **55**, 925-930.

**Apelqvist, A., Li, H., Sommer, L., Beatus, P., Anderson, D. J., Honjo, T., Hrabe de Angelis, M., Lendahl, U. and Edlund, H.** (1999). Notch signalling controls pancreatic cell differentiation. *Nature* **400**, 877-881.

**Butler, J. M., Kobayashi, H. and Rafii, S.** (2010a). Instructive role of the vascular niche in promoting tumour growth and tissue repair by angiocrine factors. *Nat. Rev. Cancer* **10**, 138-146.

**Butler, J. M., Nolan, D. J., Vertes, E. L., Varnum-Finney, B., Kobayashi, H., Hooper, A. T., Seandel, M., Shido, K., White, I. A., Kobayashi, M. et al.** (2010b). Endothelial cells are essential for the self-renewal and repopulation of Notch-dependent hematopoietic stem cells. *Cell Stem Cell* **6**, 251-264.

**Cleaver, O. and MacDonald, R. J.** (2009). Developmental molecular biology of the pancreas. In *Handbook of Pancreatic Cancer* (ed. J. Neoptolemos, J. Abbruzzese, M. Buchler and R. Urrutia). New York: Springer.

**D'Amour, K. A., Bang, A. G., Eliazer, S., Kelly, O. G., Agulnick, A. D., Smart, N. G., Moorman, M. A., Kroon, E., Carpenter, M. K. and Baetge, E. E.** (2006). Production of pancreatic hormone-expressing endocrine cells from human embryonic stem cells. *Nat. Biotechnol.* **24**, 1392-1401.

**Dor, Y., Camenisch, T. D., Itin, A., Fishman, G. I., McDonald, J. A., Carmeliet, P. and Keshet, E.** (2001). A novel role for VEGF in endocardial cushion formation and its potential contribution to congenital heart defects. *Development* **128**, 1531-1538.

**Esni, F., Ghosh, B., Biankin, A. V., Lin, J. W., Albert, M. A., Yu, X., MacDonald, R. J., Civin, C. I., Real, F. X., Pack, M. A. et al.** (2004). Notch inhibits Ptf1 function and acinar cell differentiation in developing mouse and zebrafish pancreas. *Development* **131**, 4213-4224.

**Gittes, G. K.** (2009). Developmental biology of the pancreas: a comprehensive review. *Dev. Biol.* **326**, 4-35.

**Gu, G., Wells, J. M., Dombkowski, D., Preffer, F., Aronow, B. and Melton, D. A.** (2004). Global expression analysis of gene regulatory pathways during endocrine pancreatic development. *Development* **131**, 165-179.

**Hald, J., Hjorth, J. P., German, M. S., Madsen, O. D., Serup, P. and Jensen, J.** (2003). Activated Notch1 prevents differentiation of pancreatic acinar cells and attenuate endocrine development. *Dev. Biol.* **260**, 426-437.

**Hart, A., Papadopoulou, S. and Edlund, H.** (2003). Fgf10 maintains notch activation, stimulates proliferation, and blocks differentiation of pancreatic epithelial cells. *Dev. Dyn.* **228**, 185-193.

**Holland, A. M., Hale, M. A., Kagami, H., Hammer, R. E. and MacDonald, R. J.** (2002). Experimental control of pancreatic development and maintenance. *Proc. Natl. Acad. Sci. USA* **99**, 12236-12241.

**Ilovich, O., Jacobson, O., Aviv, Y., Litchi, A., Chisin, R. and Mishani, E.** (2008). Formation of fluorine-18 labeled diaryl ureas-labeled VEGFR-2/PDGFR dual inhibitors as molecular imaging agents for angiogenesis. *Bioorg. Med. Chem.* **16**, 4242-4251.

**Jacquemin, P., Yoshitomi, H., Kashima, Y., Rousseau, G. G., Lemaigre, F. P. and Zaret, K. S.** (2006). An endothelial-mesenchymal relay pathway regulates early phases of pancreas development. *Dev. Biol.* **290**, 189-199.

**Jorgensen, M. C., Ahnfelt-Ronne, J., Hald, J., Madsen, O. D., Serup, P. and Hecksher-Sorensen, J.** (2007). An illustrated review of early pancreas development in the mouse. *Endocr. Rev.* **28**, 685-705.
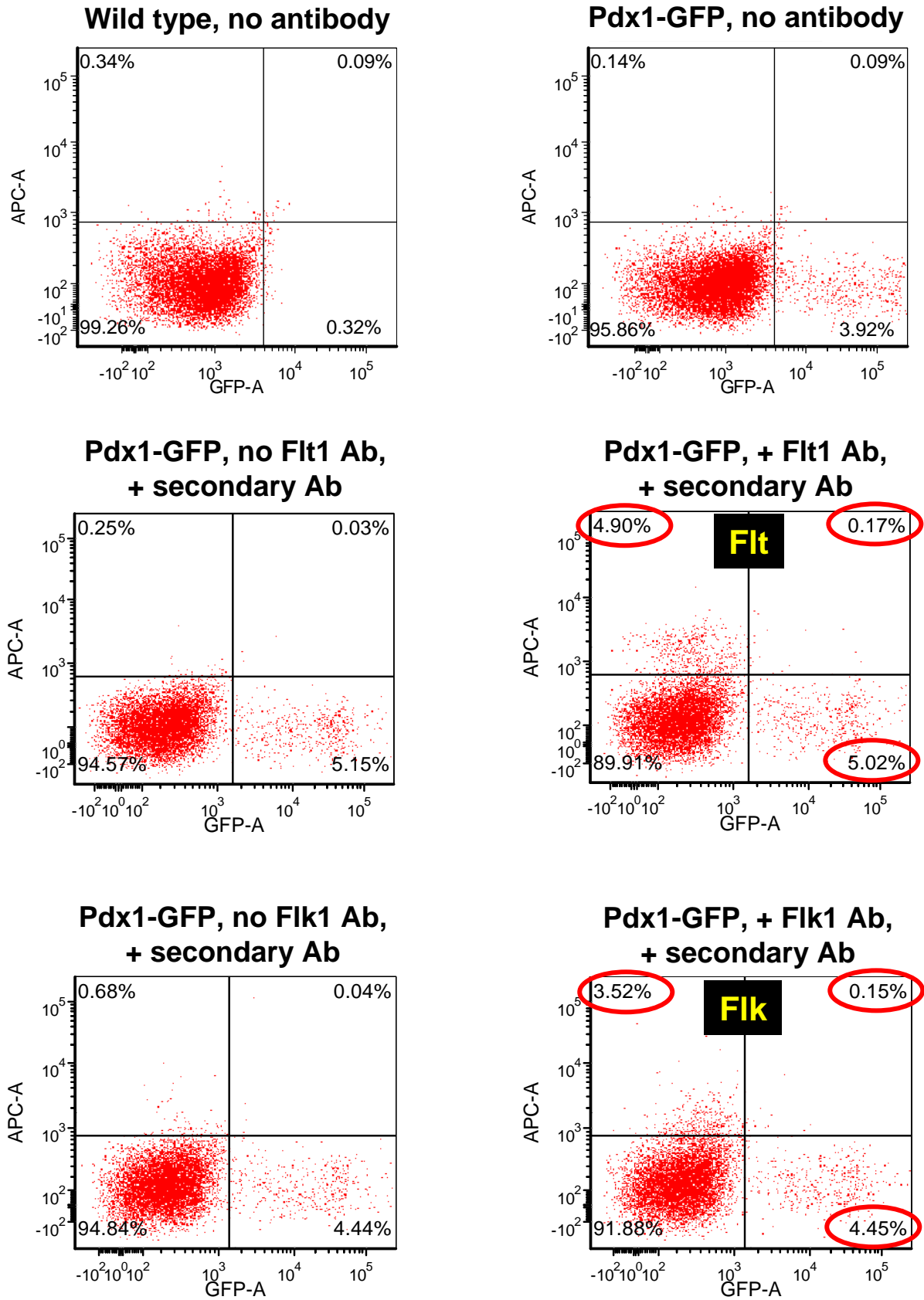
**Kesavan, G., Sand, F. W., Greiner, T. U., Johansson, J. K., Kobberup, S., Wu, X., Brakebusch, C. and Semb, H.** (2009). Cdc42-mediated tubulogenesis controls cell specification. *Cell* **139**, 791-801.

**Kroon, E., Martinson, L. A., Kadoya, K., Bang, A. G., Kelly, O. G., Eliazer, S., Young, H., Richardson, M., Smart, N. G., Cunningham, J. et al.** (2008). Pancreatic endoderm derived from human embryonic stem cells generates glucose-responsive insulin-secreting cells in vivo. *Nat. Biotechnol.* **26**, 443-452.

**Lammert, E., Cleaver, O. and Melton, D.** (2001). Induction of pancreatic differentiation by signals from blood vessels. *Science* **294**, 564-567.

**LeCouter, J., Moritz, D. R., Li, B., Phillips, G. L., Liang, X. H., Gerber, H. P., Hillan, K. J. and Ferrara, N.** (2003). Angiogenesis-independent endothelial protection of liver: role of VEGFR-1. *Science* **299**, 890-893.

**Magenheim, J., Klein, A. M., Stanger, B. Z., Ashery-Padan, A., Sosa-Pineda, B., Gu, G. and Dor, Y.** (2011). Ngn3+ endocrine progenitor cells control the fate and morphogenesis of pancreatic ductal epithelium. *Dev. Biol*. doi: 10.1016/j.ydbio.2011.08.006.

**Matsumoto, K., Yoshitomi, H., Rossant, J. and Zaret, K. S.** (2001). Liver organogenesis promoted by endothelial cells prior to vascular function. *Science* **294**, 559-563.

**May, D., Gilon, D., Djonov, V., Itin, A., Lazarus, A., Gordon, O., Rosenberger, C. and Keshet, E.** (2008). Transgenic system for conditional induction and rescue of chronic myocardial hibernation provides insights into genomic programs of hibernation. *Proc. Natl. Acad. Sci. USA* **105**, 282-287.

**Murtaugh, L. C.** (2007). Pancreas and beta-cell development: from the actual to the possible. *Development* **134**, 427-438.

**Murtaugh, L. C., Stanger, B. Z., Kwan, K. M. and Melton, D. A.** (2003). Notch signaling controls multiple steps of pancreatic differentiation. *Proc. Natl. Acad. Sci. USA* **100**, 14920-14925.

**Nikolova, G., Jabs, N., Konstantinova, I., Domogatskaya, A., Tryggvason, K., Sorokin, L., Fassler, R., Gu, G., Gerber, H. P., Ferrara, N. et al.** (2006). The vascular basement membrane: a niche for insulin gene expression and Beta cell proliferation. *Dev. Cell* **10**, 397-405.

**Norgaard, G. A., Jensen, J. N. and Jensen, J.** (2003). FGF10 signaling maintains the pancreatic progenitor cell state revealing a novel role of Notch in organ development. *Dev. Biol.* **264**, 323-338.

**Oliver-Krasinski, J. M. and Stoffers, D. A.** (2008). On the origin of the beta cell. *Genes Dev.* **22**, 1998-2021.

**Palmer, T. D., Willhoite, A. R. and Gage, F. H.** (2000). Vascular niche for adult hippocampal neurogenesis. *J. Comp. Neurol.* **425**, 479-494.

**Pierreux, C. E., Cordi, S., Hick, A. C., Achouri, Y., Ruiz de Almodovar, C., Prevot, P. P., Courtoy, P. J., Carmeliet, P. and Lemaigre, F. P.** (2010). Epithelial: Endothelial cross-talk regulates exocrine differentiation in developing pancreas. *Dev. Biol.* **347**, 216-227.

**Puri, S. and Hebrok, M.** (2007). Dynamics of embryonic pancreas development using real-time imaging. *Dev. Biol.* **306**, 82-93.

**Sand, F. W., Hornblad, A., Johansson, J. K., Loren, C., Edsbagge, J., Stahlberg, A., Magenheim, J., Ilovich, O., Mishani, E., Dor, Y. et al.** (2011). Growth-limiting role of endothelial cells in endoderm development. *Dev. Biol.* **352**, 267-277.

**Shalaby, F., Ho, J., Stanford, W. L., Fischer, K. D., Schuh, A. C., Schwartz, L., Bernstein, A. and Rossant, J.** (1997). A requirement for Flk1 in primitive and definitive hematopoiesis and vasculogenesis. *Cell* **89**, 981-990.

**Shen, Q., Goderie, S. K., Jin, L., Karanth, N., Sun, Y., Abramova, N., Vincent, P., Pumiglia, K. and Temple, S.** (2004). Endothelial cells stimulate self-renewal and expand neurogenesis of neural stem cells. *Science* **304**, 1338-1340.

**Shen, Q., Wang, Y., Kokovay, E., Lin, G., Chuang, S. M., Goderie, S. K., Roysam, B. and Temple, S.** (2008). Adult SVZ stem cells lie in a vascular niche: a quantitative analysis of niche cell-cell interactions. *Cell Stem Cell* **3**, 289-300.

**Solar, M., Cardalda, C., Houbracken, I., Martin, M., Maestro, M. A., De Medts, N., Xu, X., Grau, V., Heimberg, H., Bouwens, L. et al.** (2009). Pancreatic exocrine duct cells give rise to insulin-producing beta cells during embryogenesis but not after birth. *Dev. Cell* **17**, 849-860.

**Tang, W., Zeve, D., Suh, J. M., Bosnakovski, D., Kyba, M., Hammer, R. E., Tallquist, M. D. and Graff, J. M.** (2008). White fat progenitor cells reside in the adipose vasculature. *Science* **322**, 583-586.

**Tavazoie, M., Van der Veken, L., Silva-Vargas, V., Louissaint, M., Colonna, L., Zaidi, B., Garcia-Verdugo, J. M. and Doetsch, F.** (2008). A specialized vascular niche for adult neural stem cells. *Cell Stem Cell* **3**, 279-288.

**van Eyll, J. M., Pierreux, C. E., Lemaigre, F. P. and Rousseau, G. G.** (2004). Shh-dependent differentiation of intestinal tissue from embryonic pancreas by activin A. *J. Cell Sci.* **117**, 2077-2086.

**Yoshida, S., Sukeno, M. and Nabeshima, Y.** (2007). A vasculature-associated niche for undifferentiated spermatogonia in the mouse testis. *Science* **317**, 1722-1726.

**Yoshitomi, H. and Zaret, K. S.** (2004). Endothelial cell interactions initiate dorsal pancreas development by selectively inducing the transcription factor Ptf1a. *Development* **131**, 807-817.

**Zaret, K. S.** (2006). Pancreatic beta cells: responding to the matrix. *Cell Metab.* **3**, 148-150.

**Zaret, K. S. and Grompe, M.** (2008). Generation and regeneration of cells of the liver and pancreas. *Science* **322**, 1490-1494.

**Zhou, Q., Law, A. C., Rajagopal, J., Anderson, W. J., Gray, P. A. and Melton, D. A.** (2007). A multipotent progenitor domain guides pancreatic organogenesis. *Dev. Cell* **13**, 103-114.

Sup. Figure 1S

E15.5: pdx1-GFP / Flk1and Flt1 staining

A

B    Similar expression patterns of Flk1 and Pecam



**Pdx1**
**Pecam**
**Flk1**

Pdx1

Pecam

Flk1

**Flk-LacZ**

**Pecam**

## Sup. Figure 2S



Effect of hypervascularization on explant size

p=0.00037

Muc1+ area

1

0.75

0.5

0.25

0

n=8

n=7

TET-VEGF

Pdx1-tTA;
TET-VEGF



TET-VEGF

Pdx1-tTA;
TET-VEGF

Experiment 1

Experiment 2

Muc1
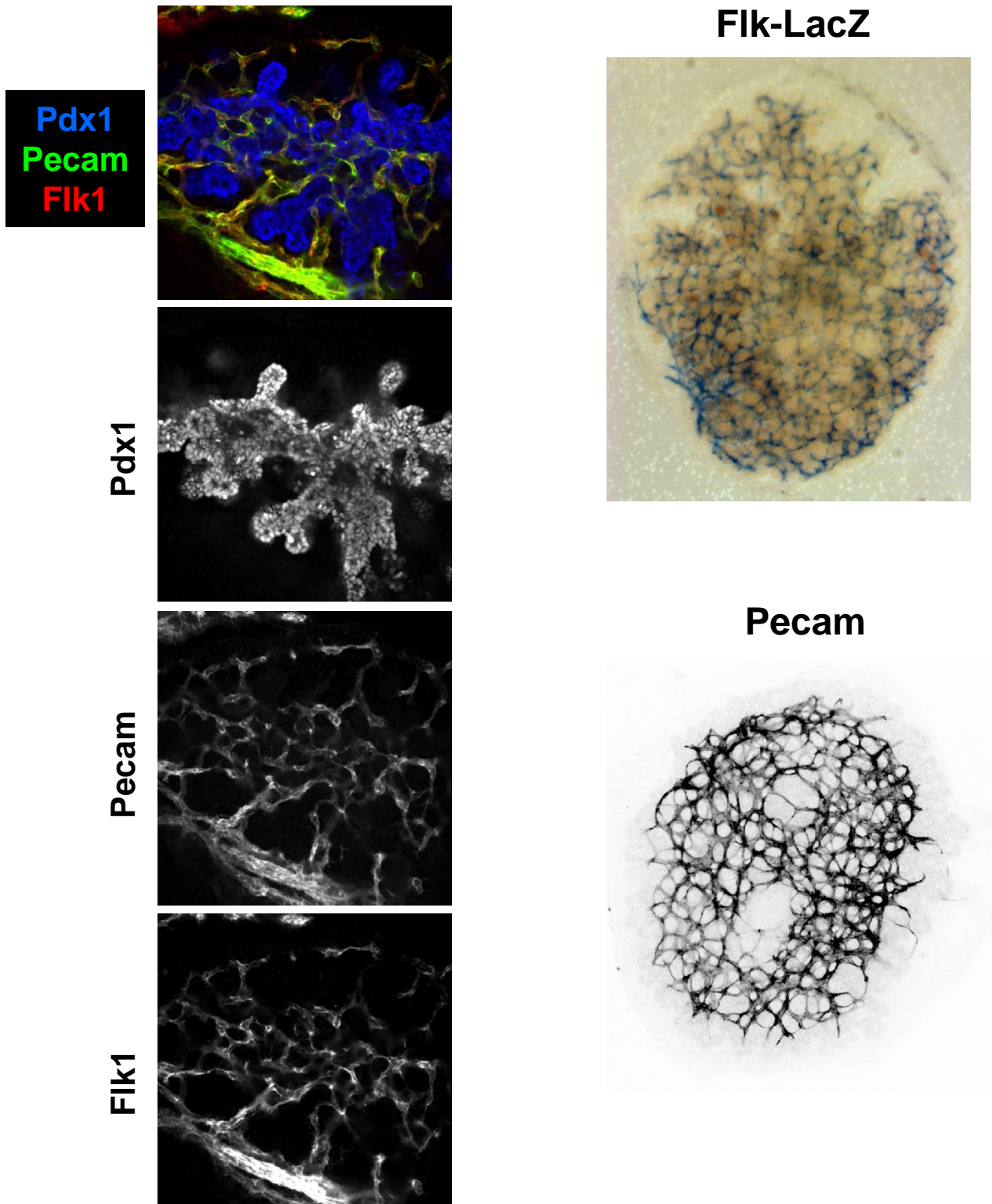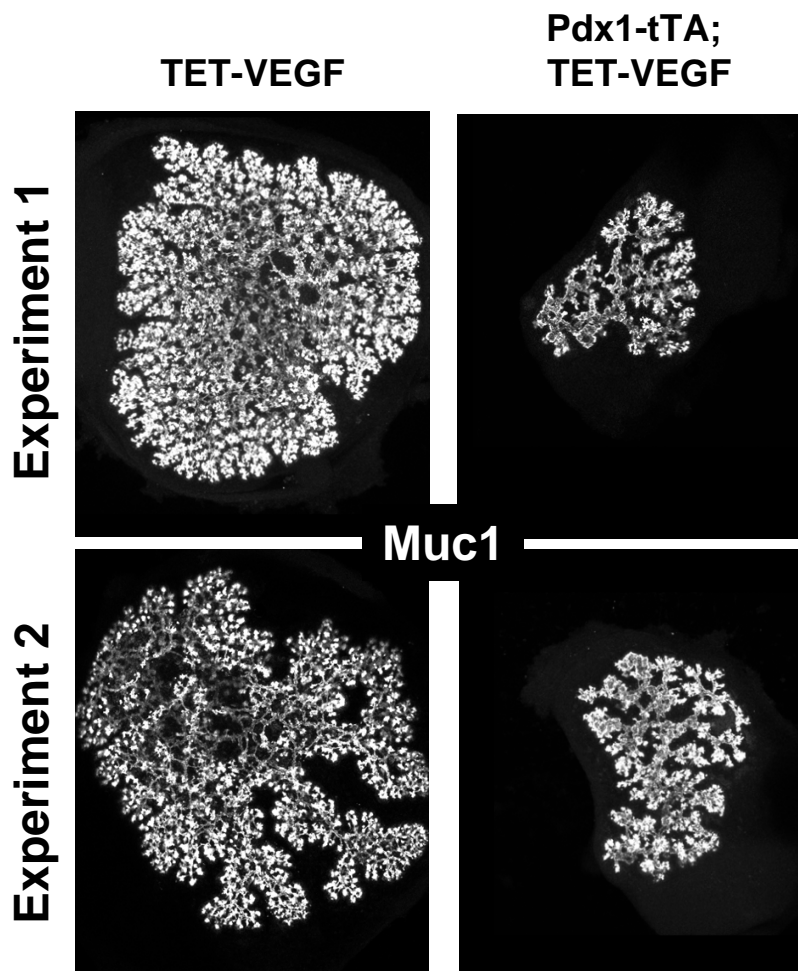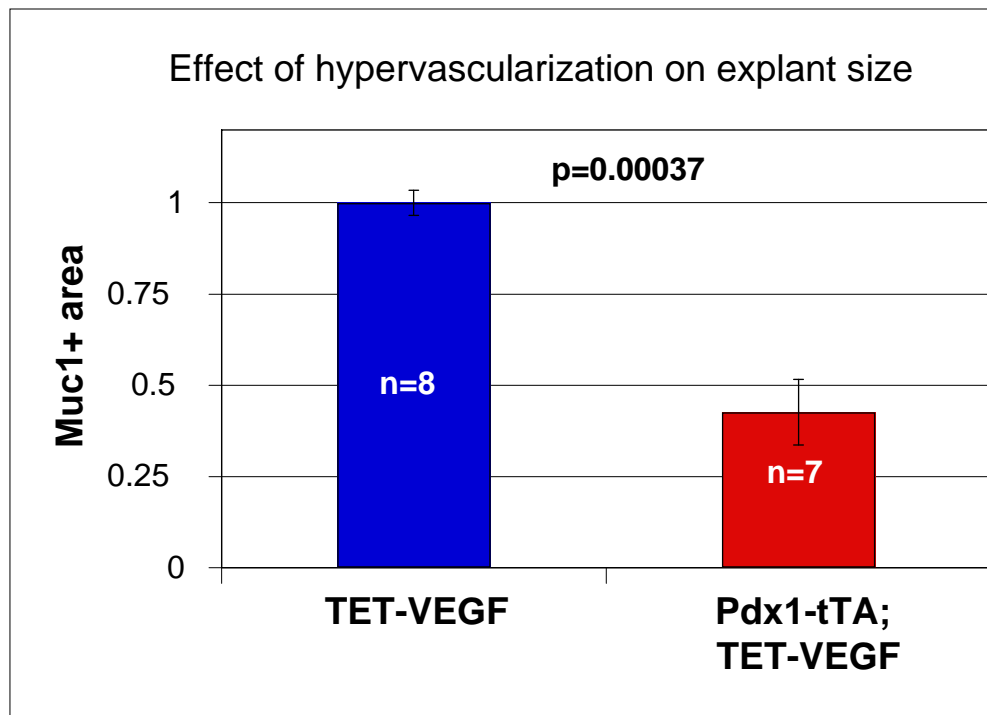
# control



Pdx1
Pecam

# VEGFRi



Pdx1
Pecam

# # slices (Z axis)

# Sup. Figure 4S

A
Control    Pdx1-tTA;TET-sFLT1

Pecam Pdx1

B
TET-sFLT1    Pdx1-tTA;
TET-sFLT1

e11.5

Pdx-1 Hypoxia Nuclei

e12.5

C
TET-sFLT1    Pdx1-tTA;
TET-sFLT1

Insulin

D
TET-sFLT1    Pdx1-tTA;
TET-sFLT1

Caspase3

Tunel Insulin DNA

## Sup. Figure 5S



**Vascular ablation and explant size**

Area (y-axis: 0, 0.5, 1, 1.5, 2)

p=0.03  *

n=8 (TET-SFlt)  n=8 (Pdx1-tTA; TET-SFlt)

TET- sFLT1    Pdx-tTA, TET-sFLT1
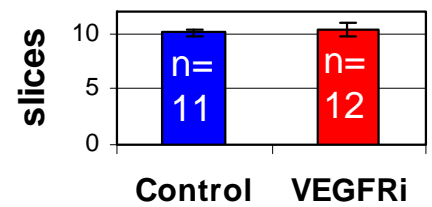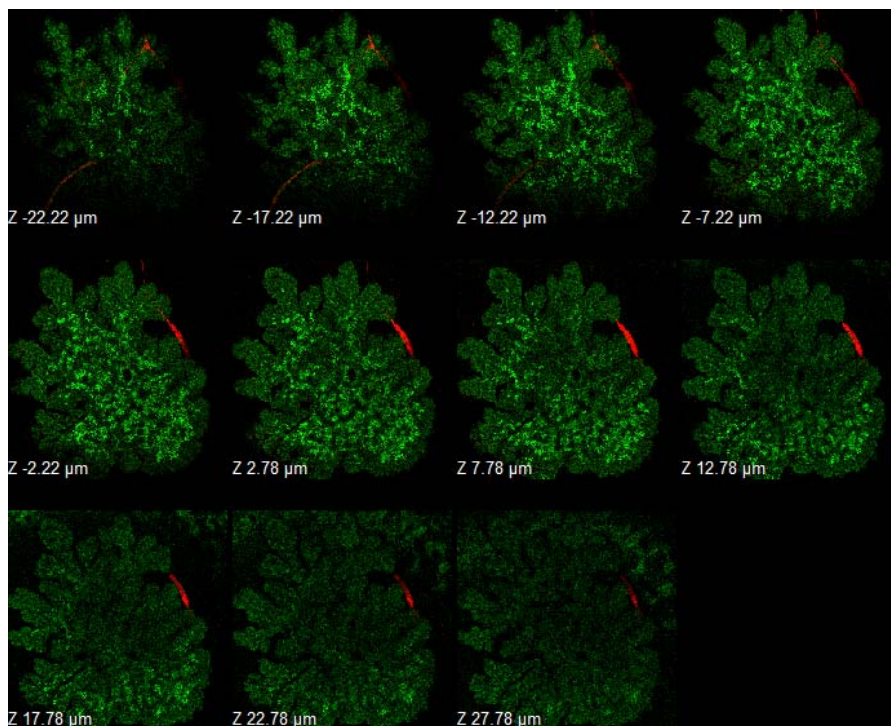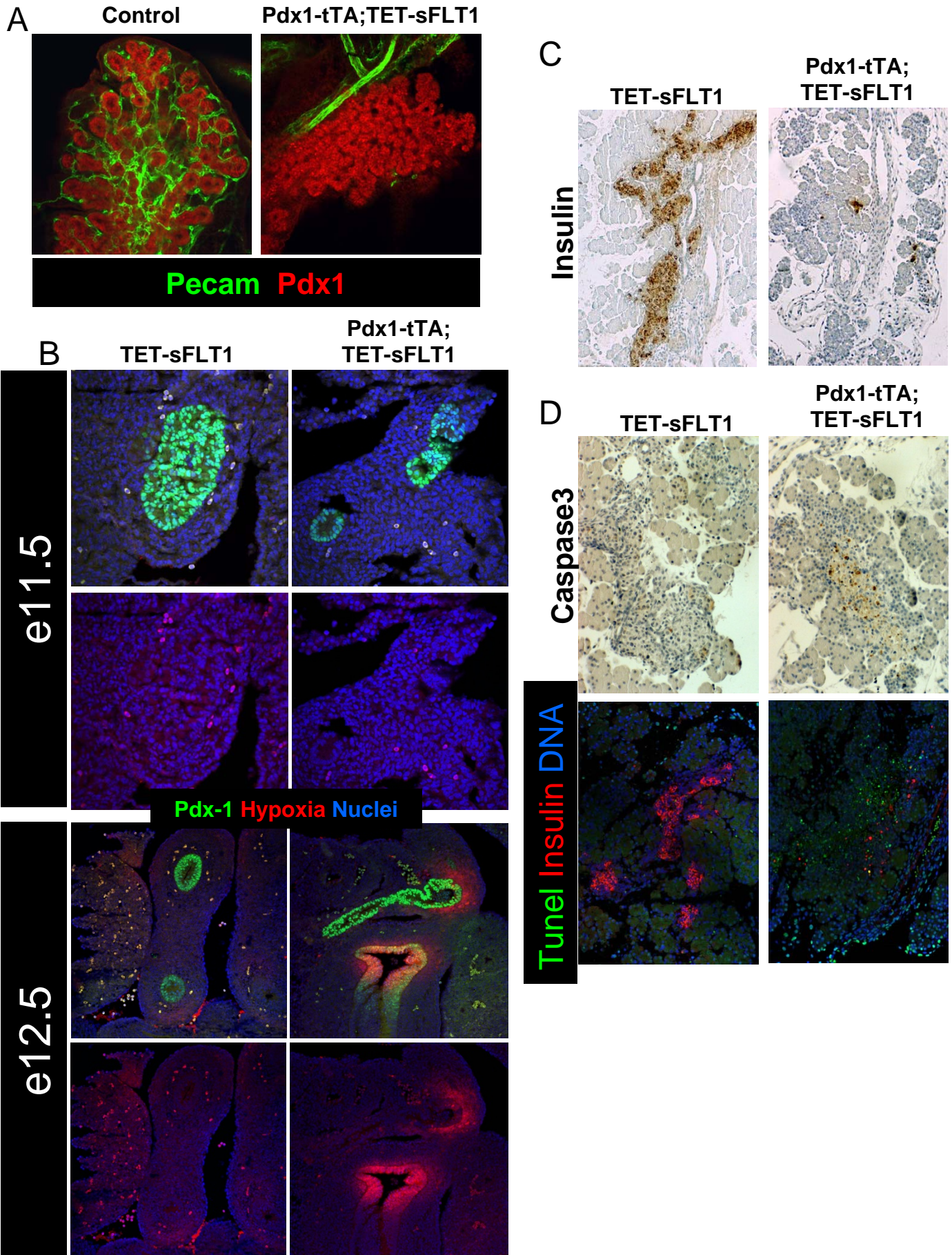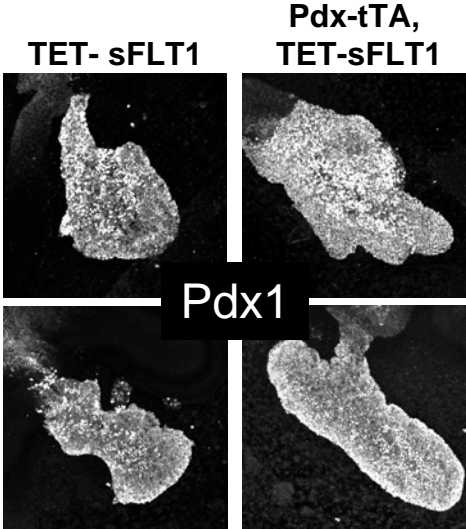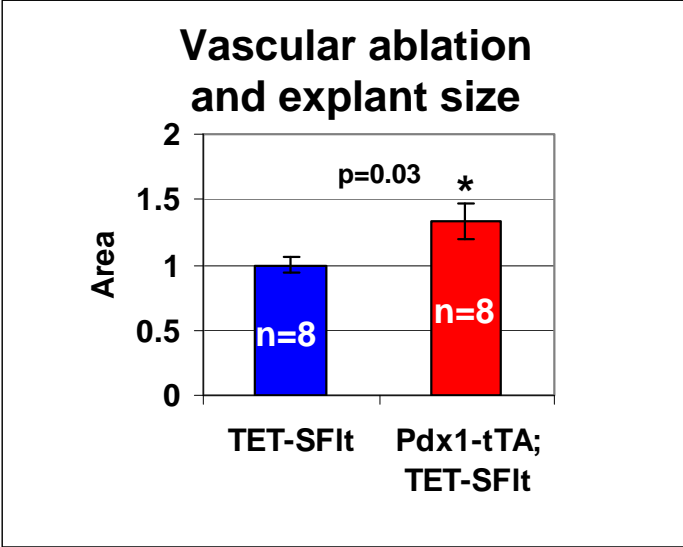
Pdx1

# Sup. Figure 6S    Tile images of Pdx1 and Ptf1a

A



Pdx1
Ptf1a

Pdx1

Ptf1a

Tile images of Pdx1 and Cpa1

B

**Merge**

Pdx1

Z -141.16 μm    Z -136.16 μm    Z -131.16 μm    Z -126.16 μm

Z -121.16 μm    Z -116.16 μm    Z -111.16 μm    Z -106.16 μm

Z -101.16 μm    Z -96.16 μm    Z -91.16 μm    Z -86.16 μm

**Pdx1-tTA**

Z=12 slices

**Merge**

Cpa1

Z -141.16 μm    Z -136.16 μm    Z -131.16 μm    Z -126.16 μm

Z -121.16 μm    Z -116.16 μm    Z -111.16 μm    Z -106.16 μm

Z -101.16 μm    Z -96.16 μm    Z -91.16 μm    Z -86.16 μm
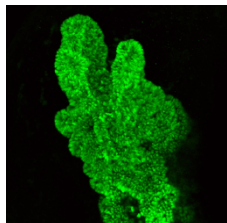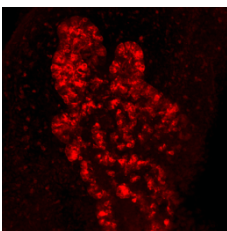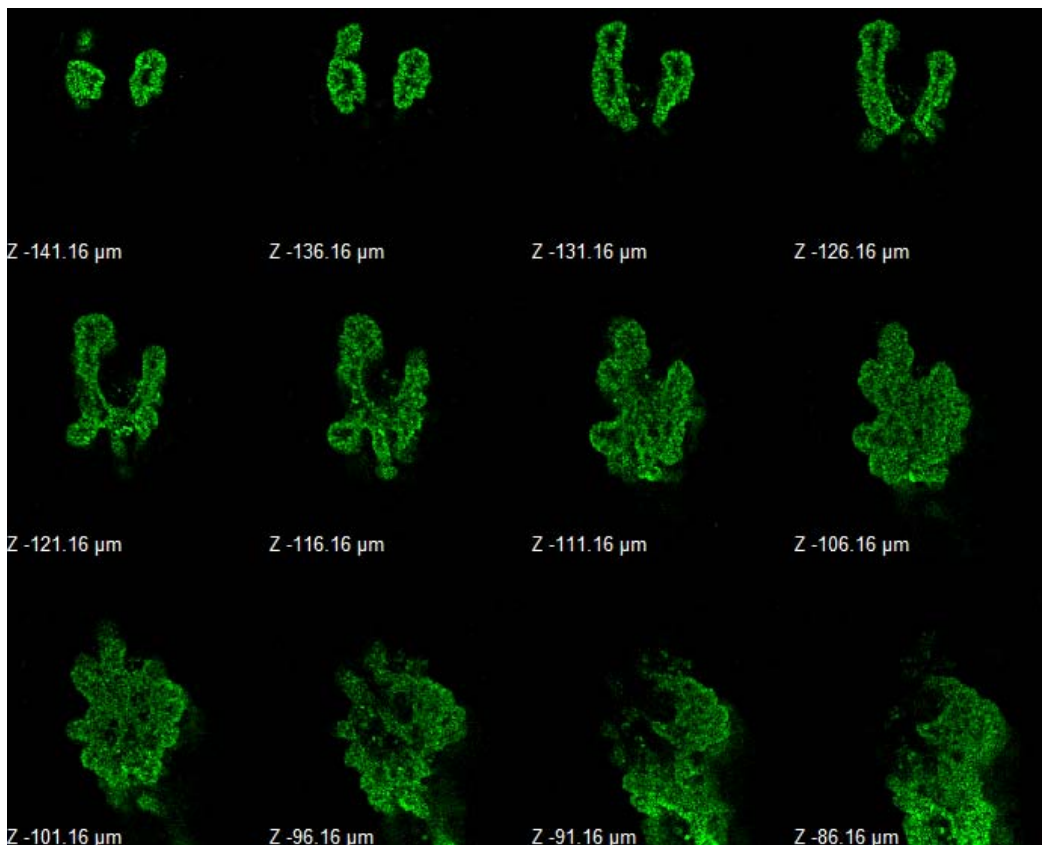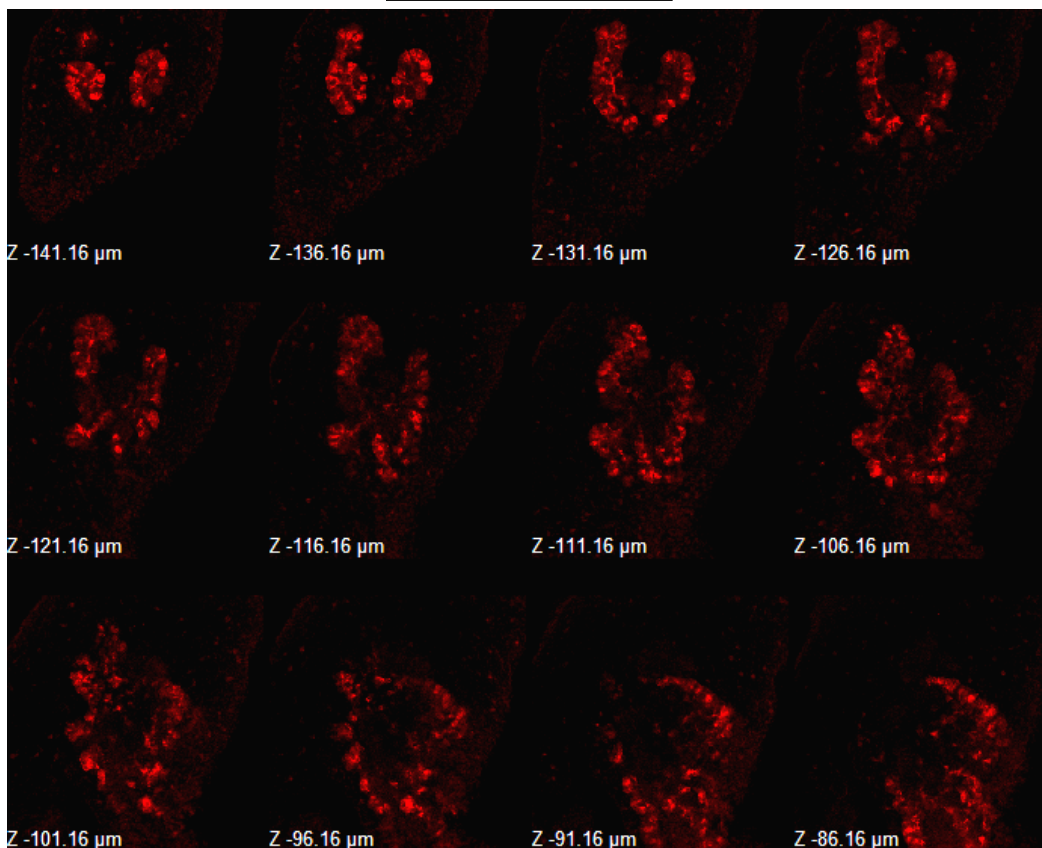
## Amylase expression in wild type
### One slice

**e12.5**                    **e15.5**
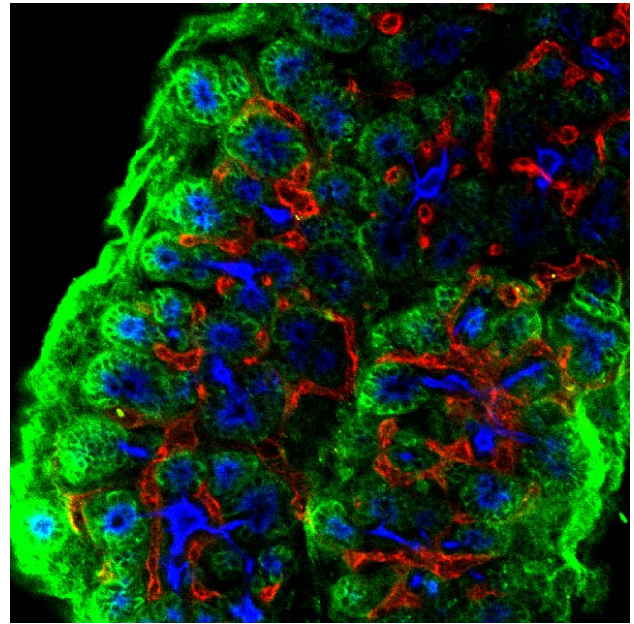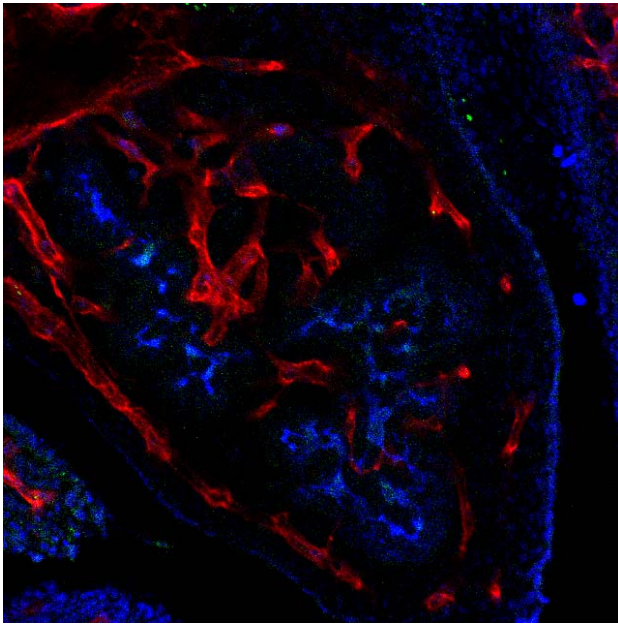


**Amylase Muc1 Pecam**
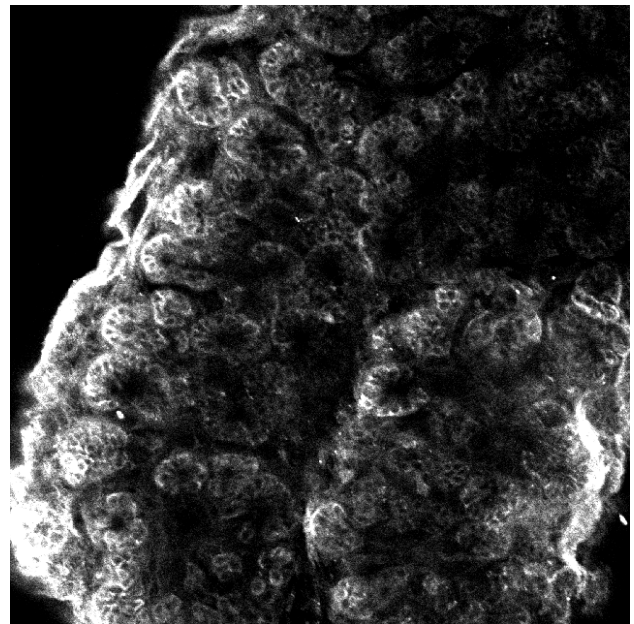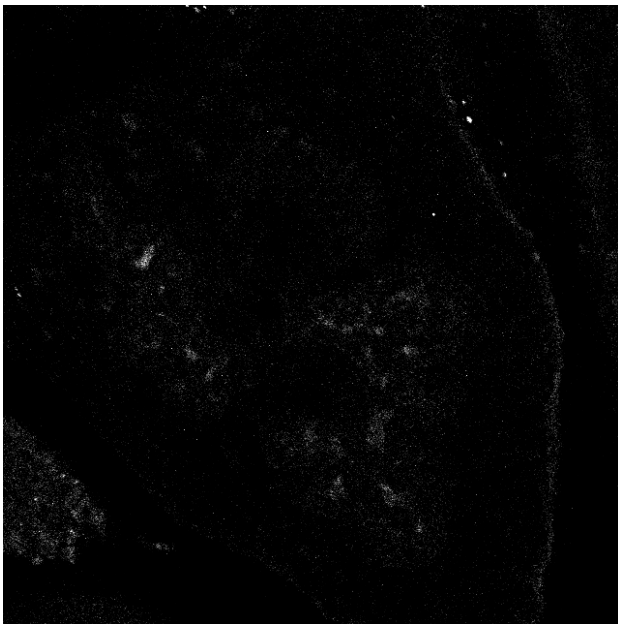
**Amylase**

Sup Figure 8S

TET-VEGF

Pdx1-tTA;
TET-VEGF

A
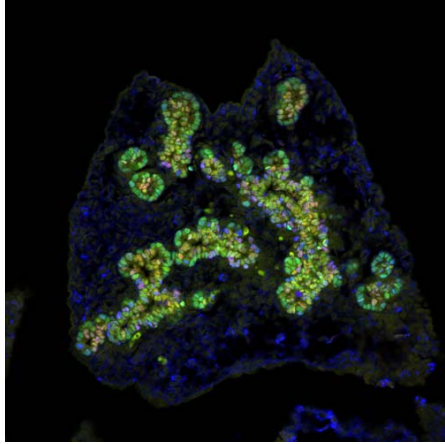
Pdx1
Nkx2.2
Nkx6.1

Pdx1

Nkx2.2

Nkx6.1

B

**E18.5**

P1

C
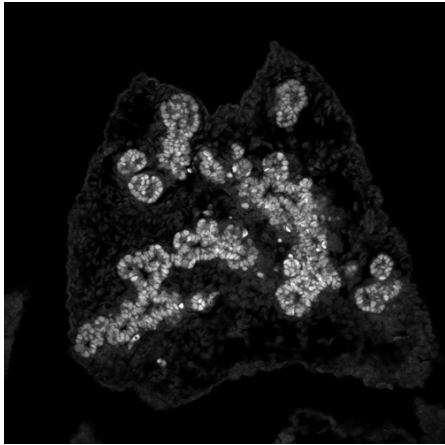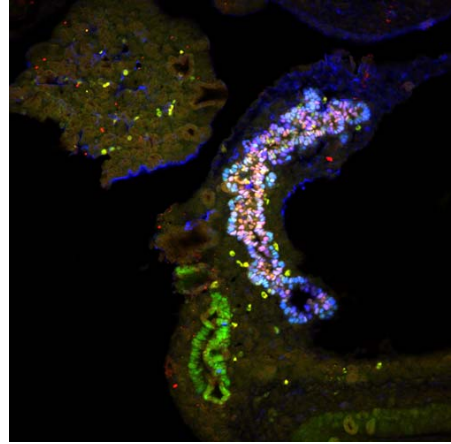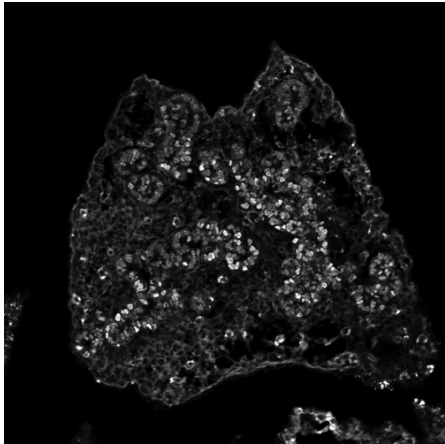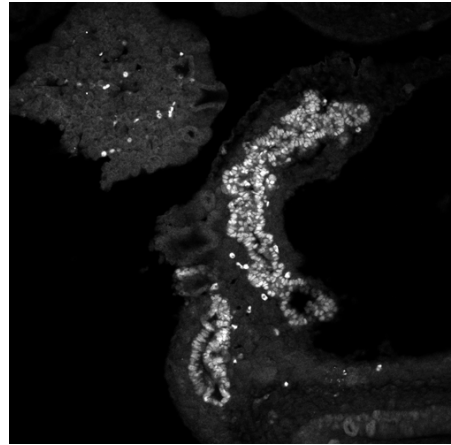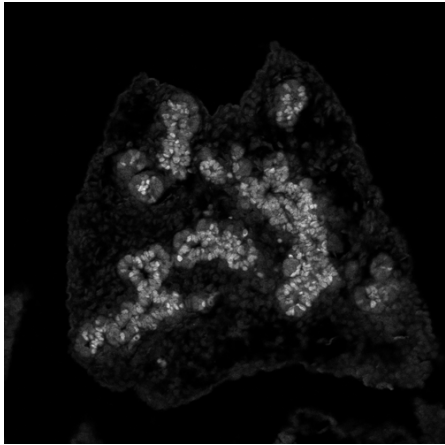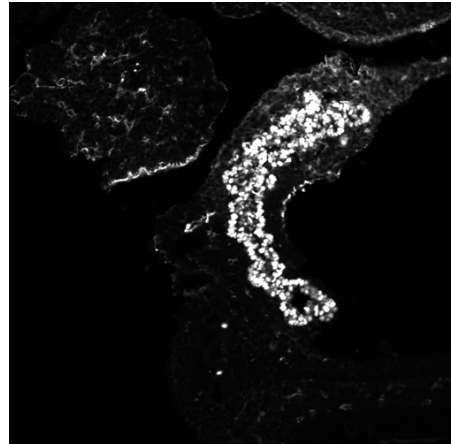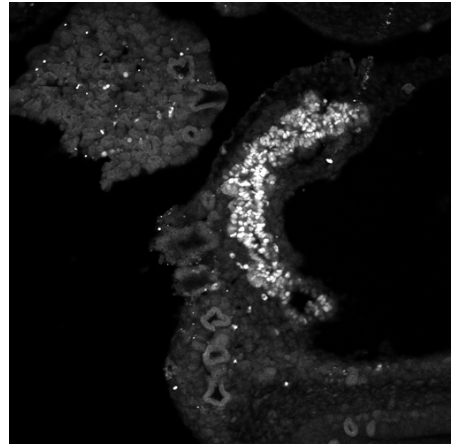
CK19
Insulin
Nkx6.1

CK19

Control

VEGF Transgenic

2 months

D
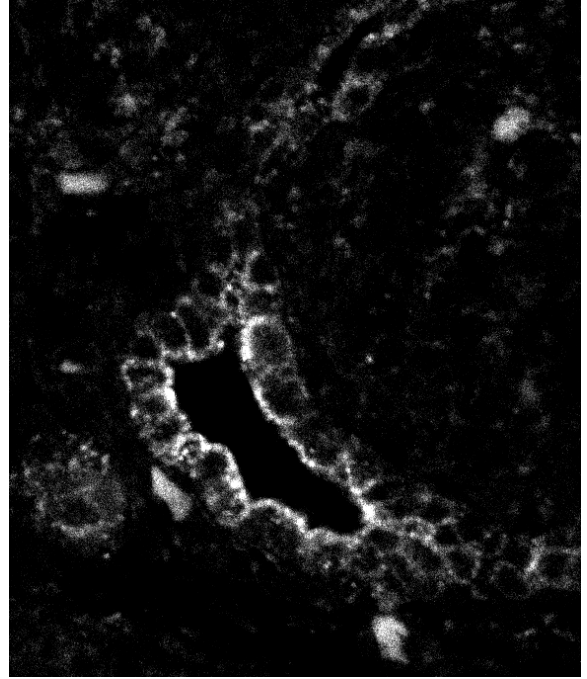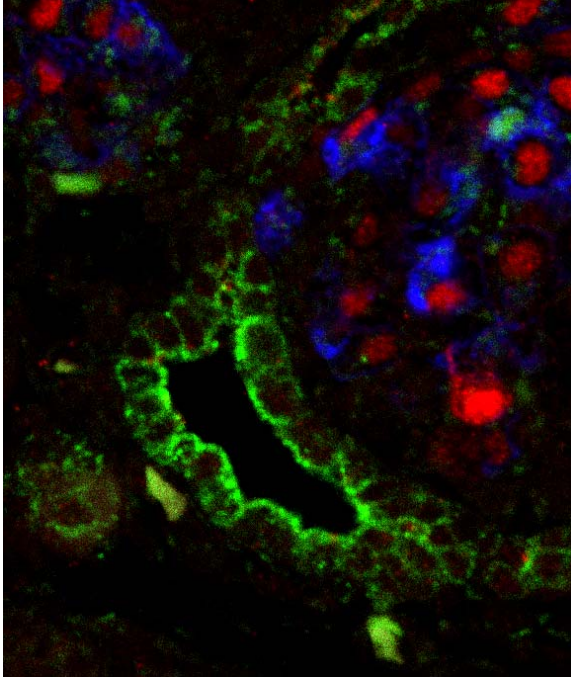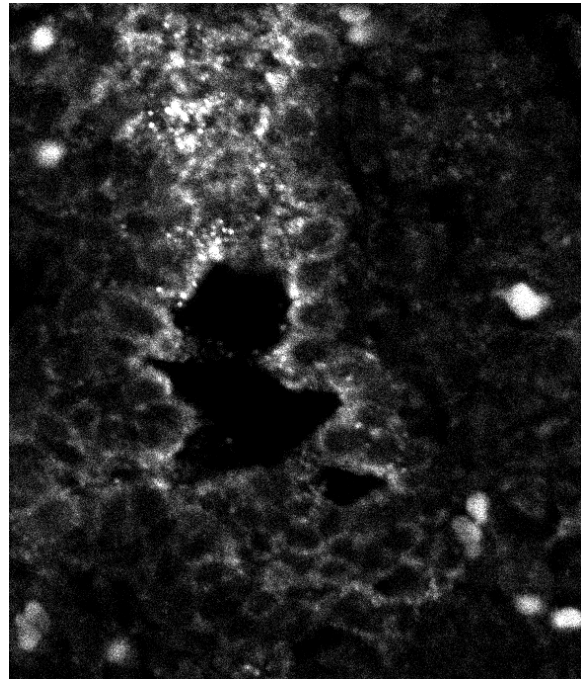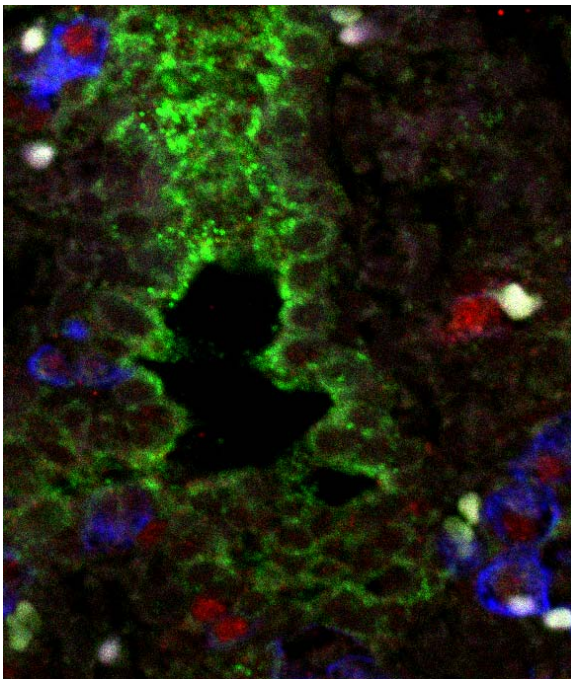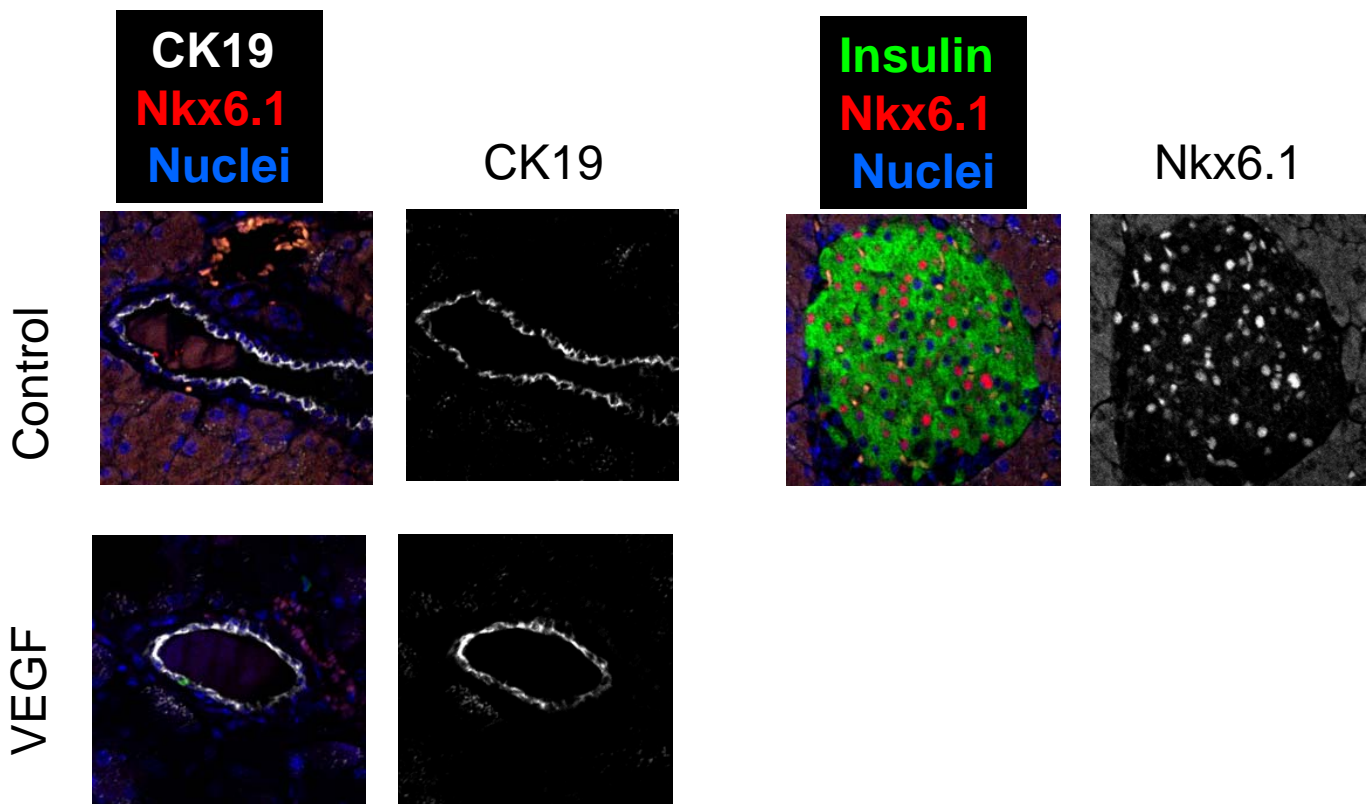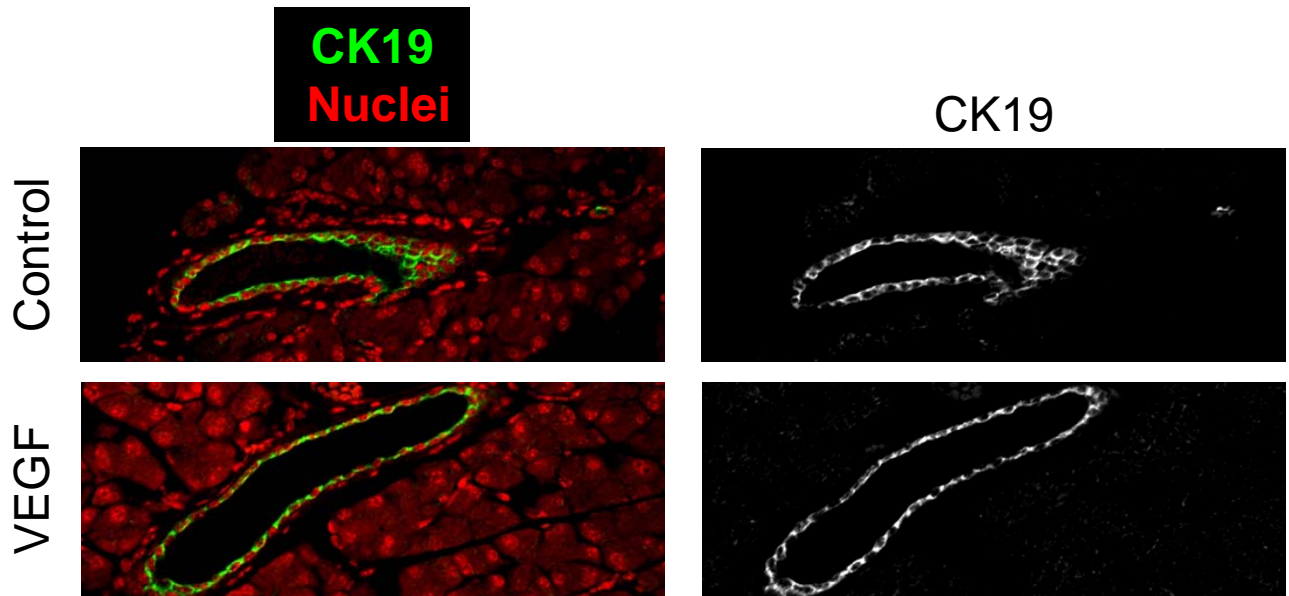
# Microarray analysis
# Summary

## VEGF overexpression: fold change over control
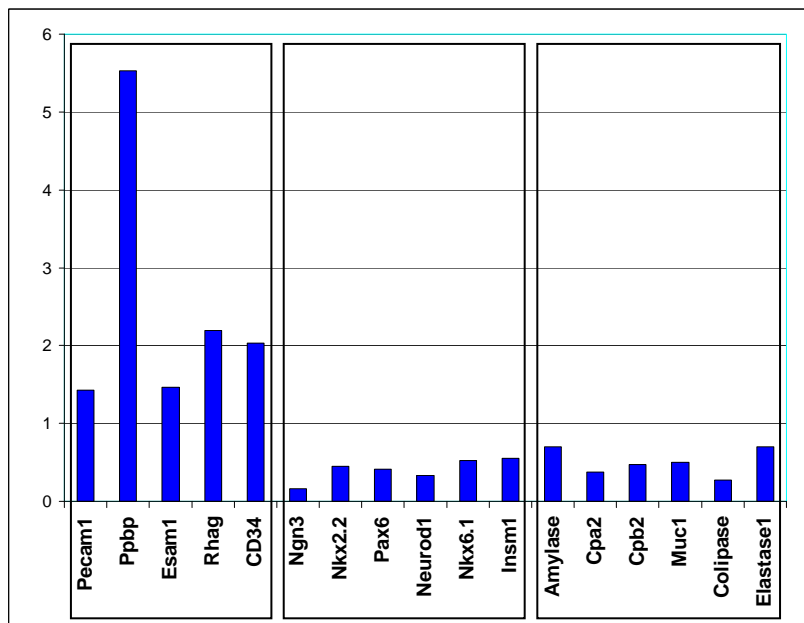


## Vascular ablation: fold change over control
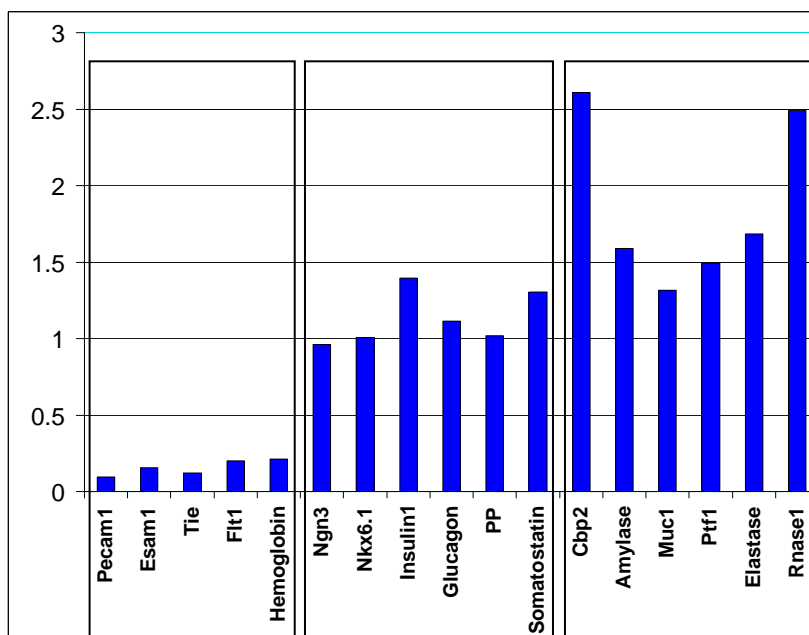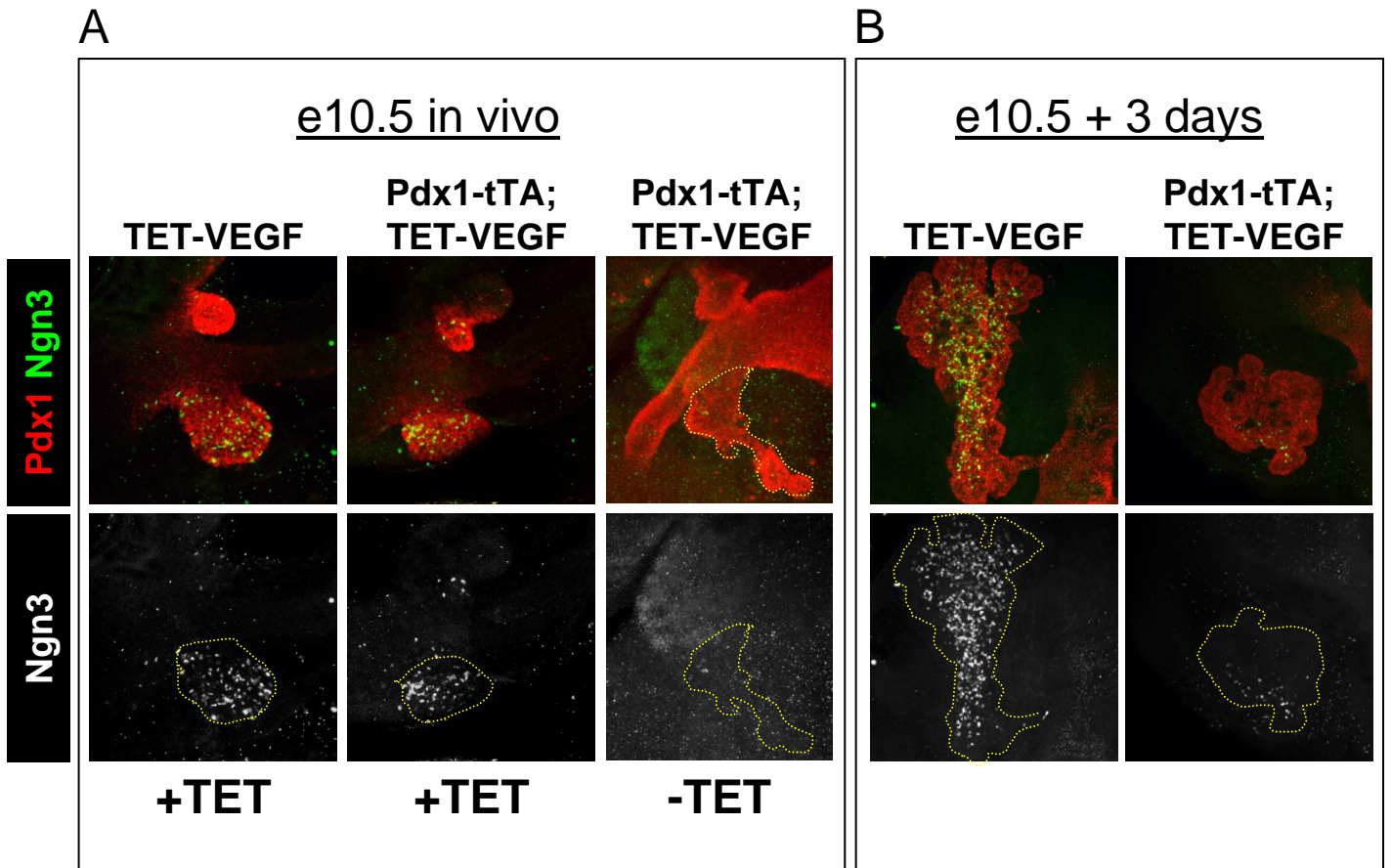
Sup Figure 10S

Wild type e12.5 explants +3 days culture



**Muc1**
**Ptf1a**

**Muc1**
**Cpa1**

Muc1

Muc1

Ptf1a
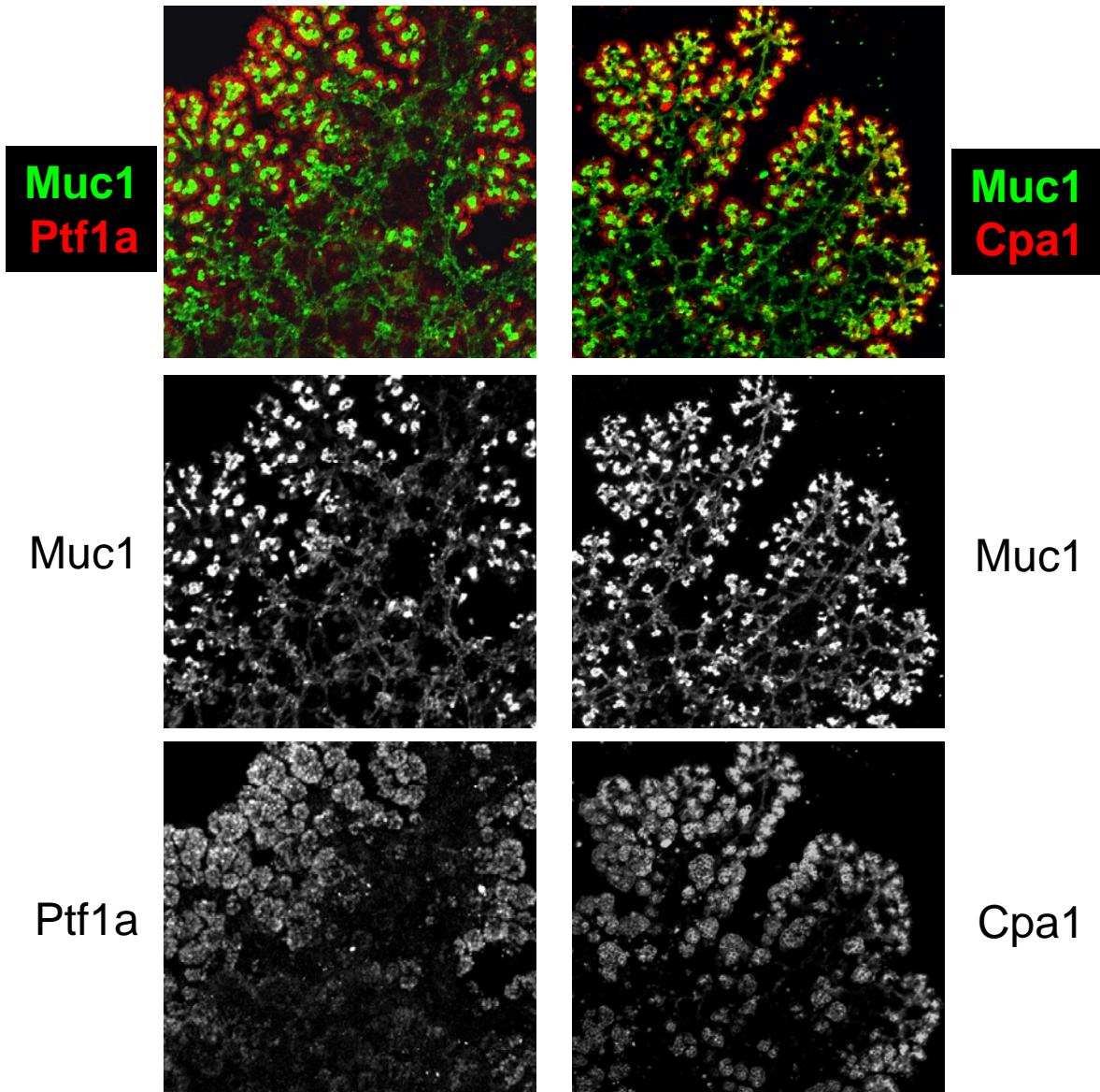
Cpa1

CPA1

Control

VEGFR2i

Z-stack
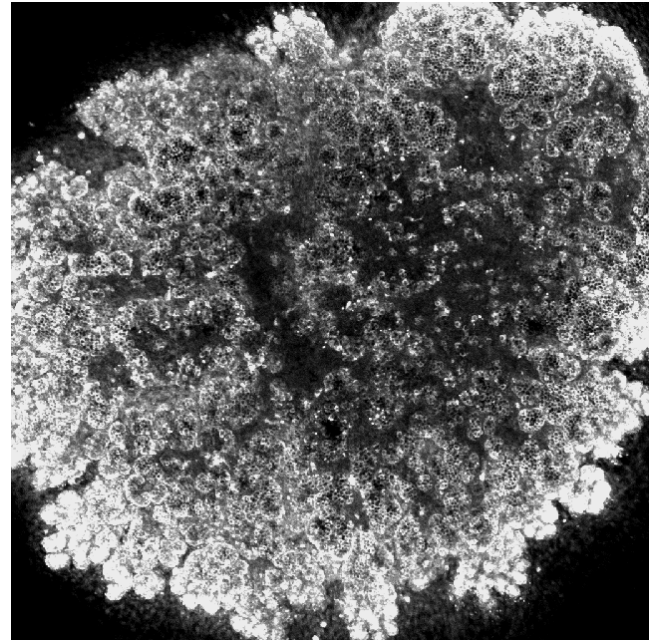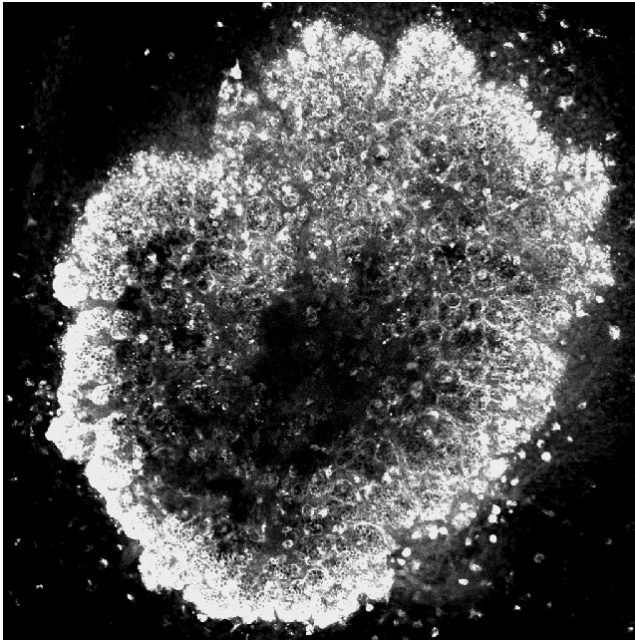
One slice
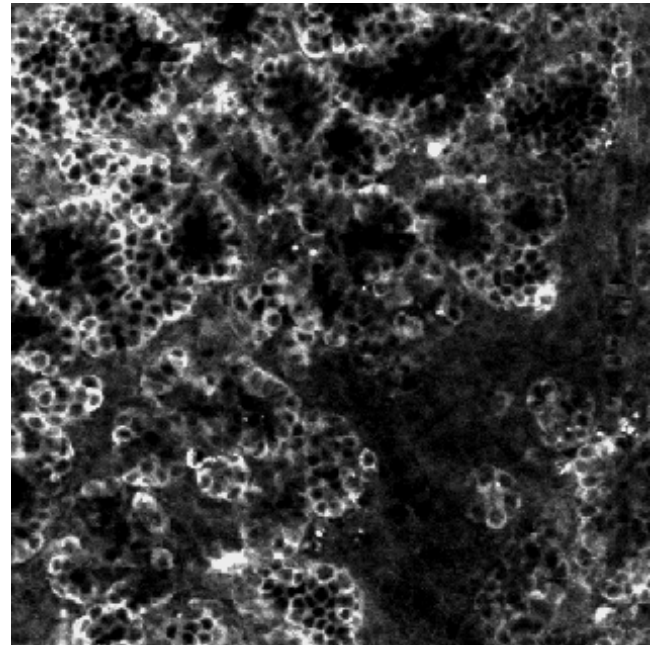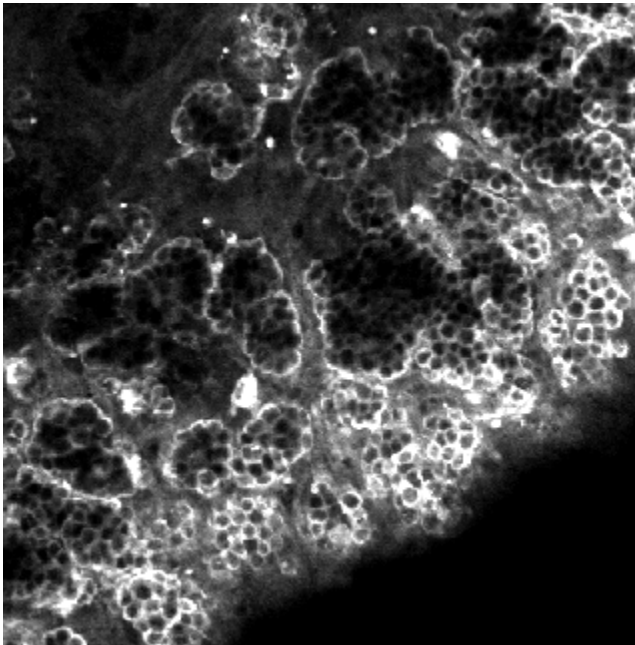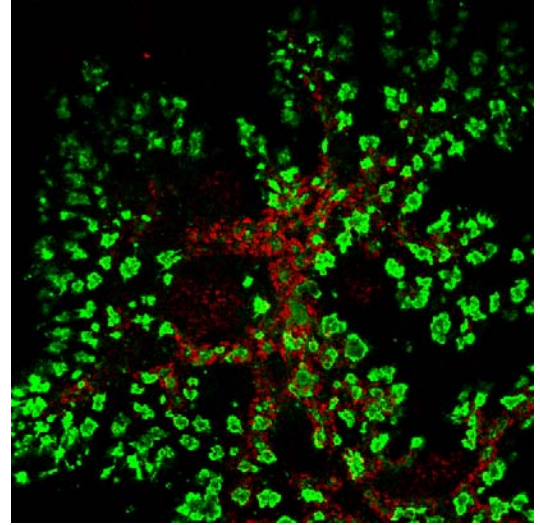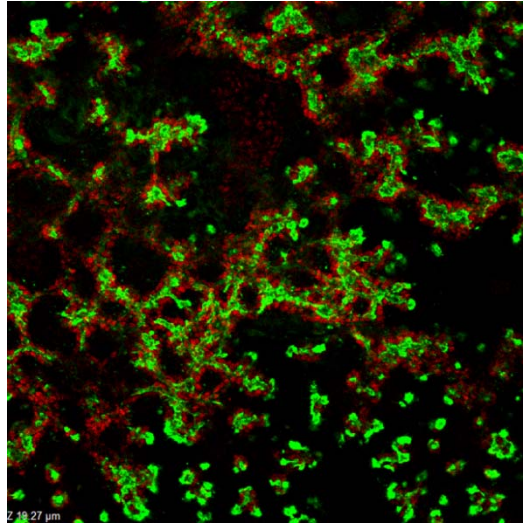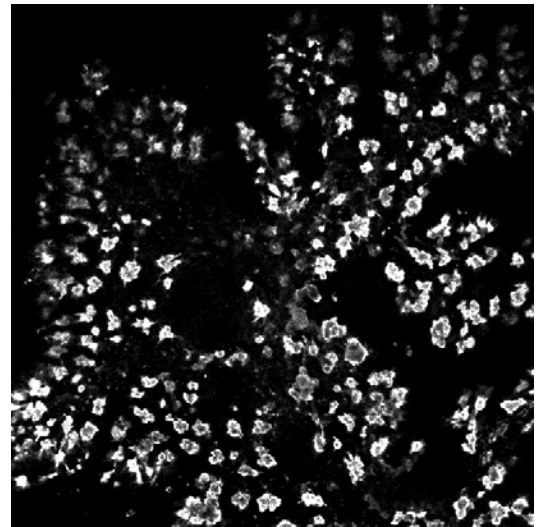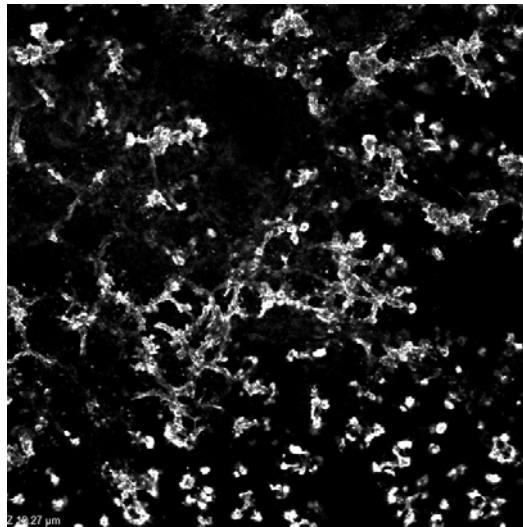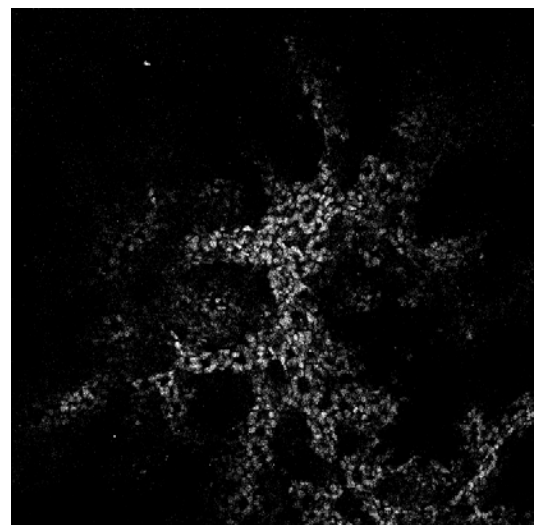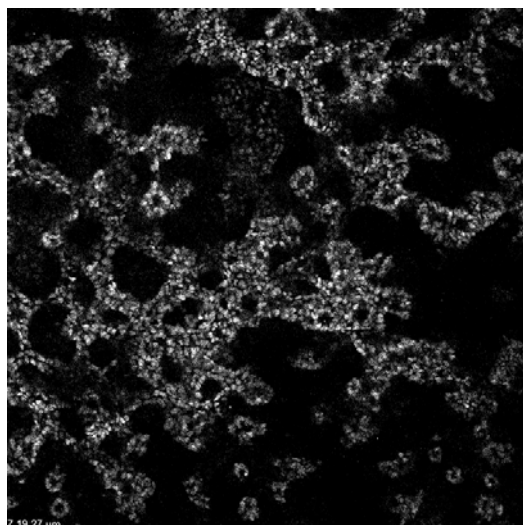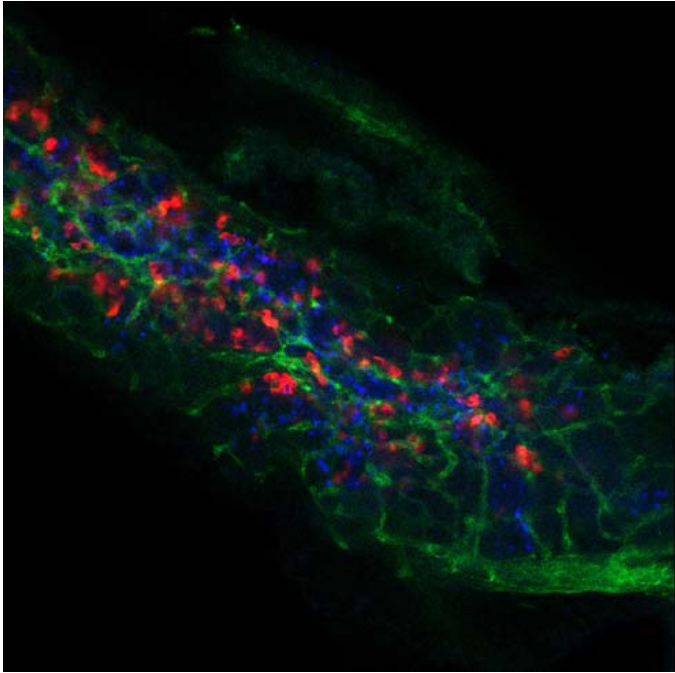
**Pdx-tTA**

**Pdx-tTA, TET-VEGF**
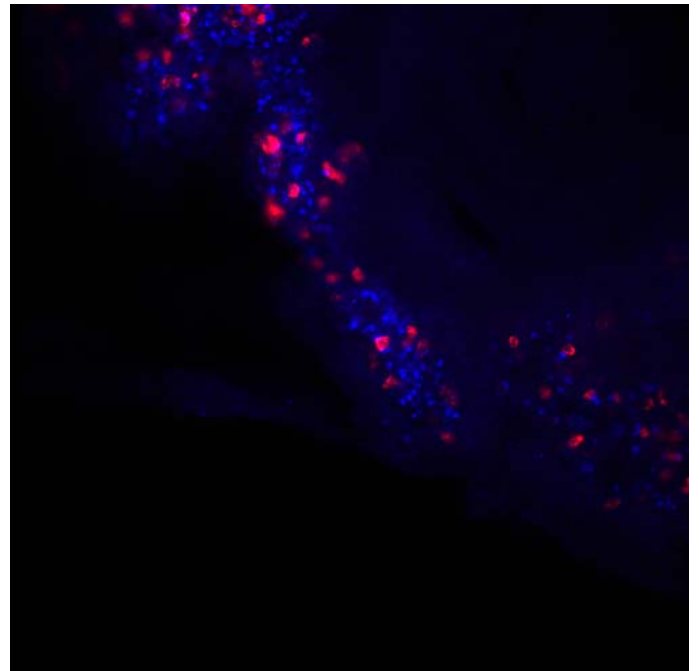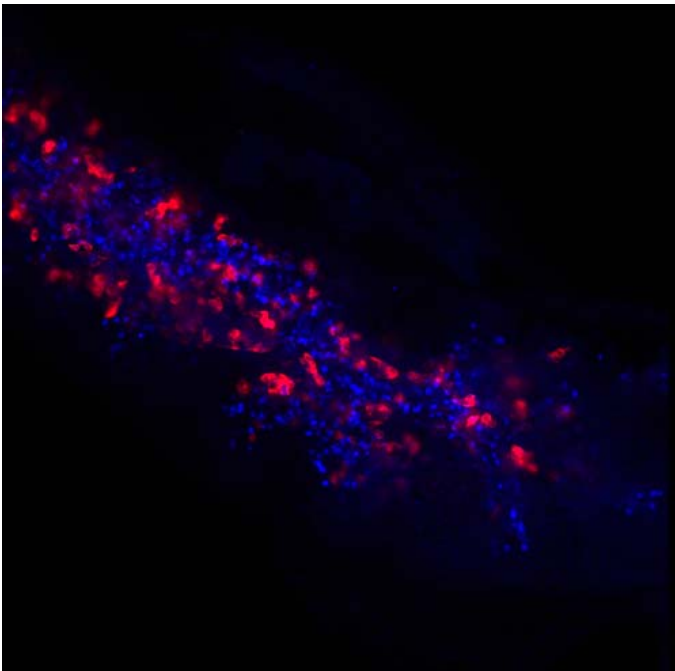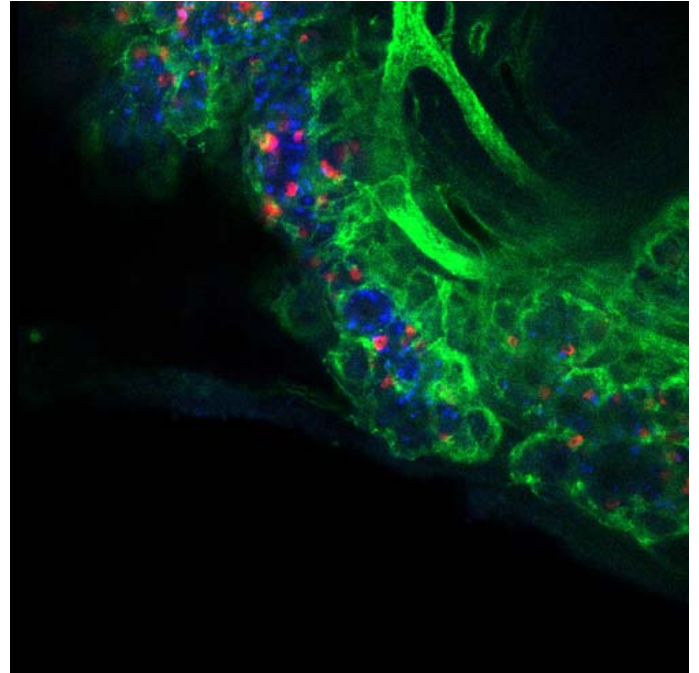


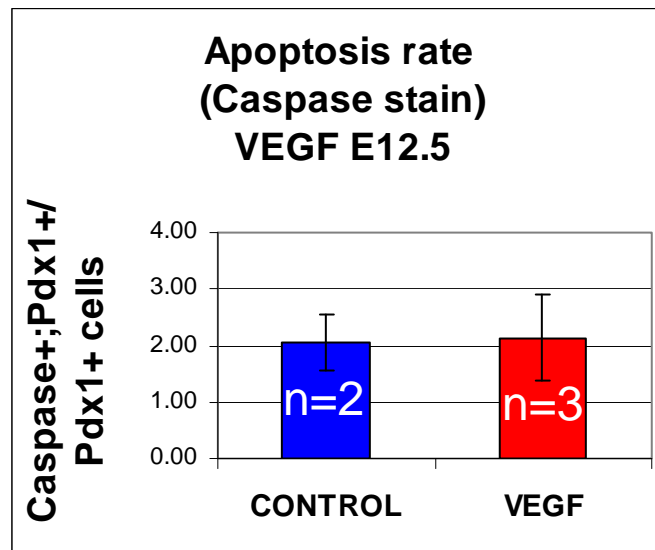**Insulin Pecam Ngn3**
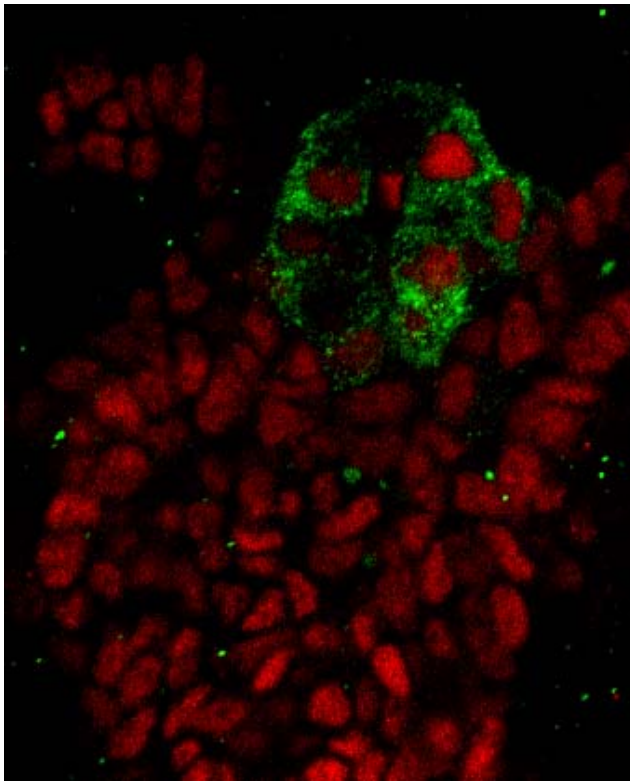
In vivo proliferation

A
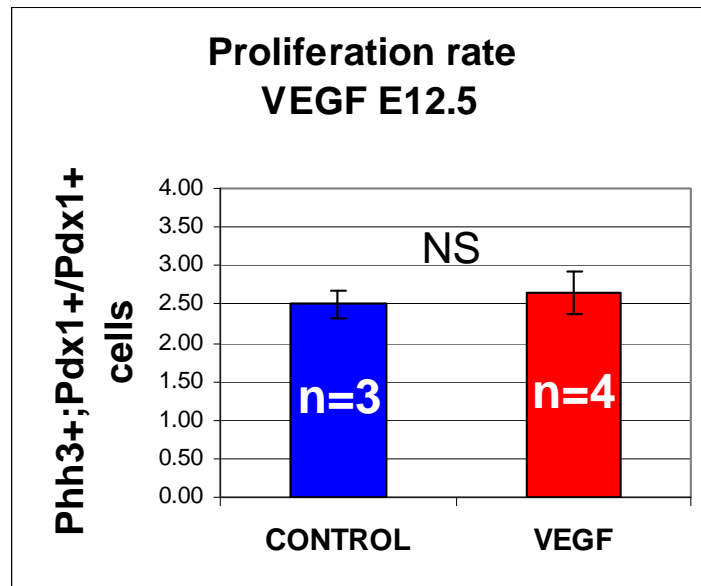


Control
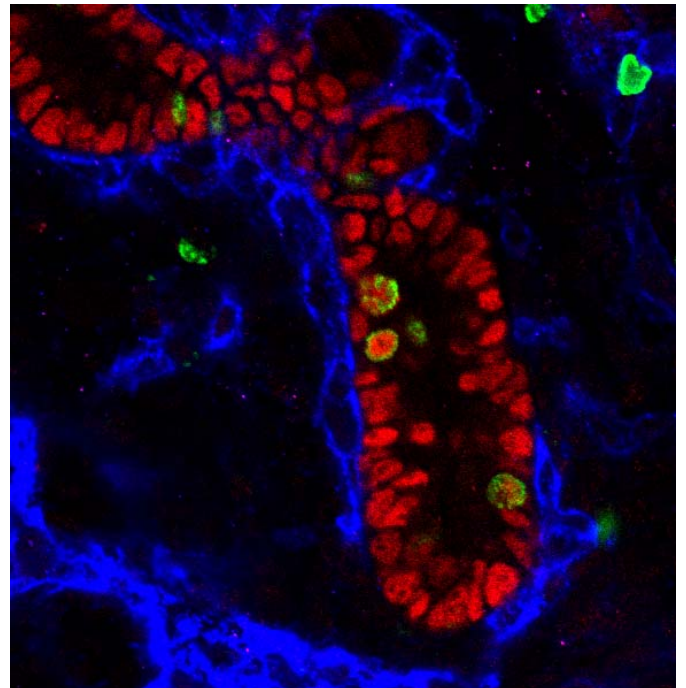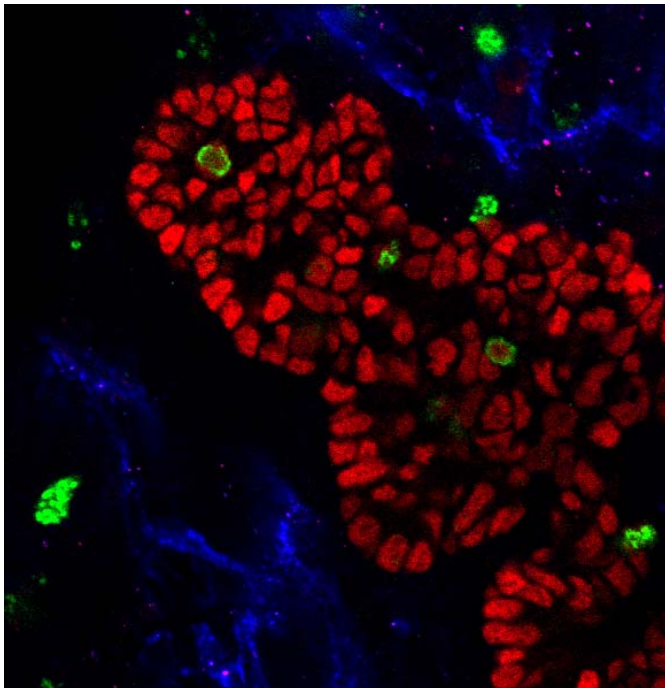
VEGF

E12.5 Pdx1 Phh3 Pecam

In vivo Apoptosis

B
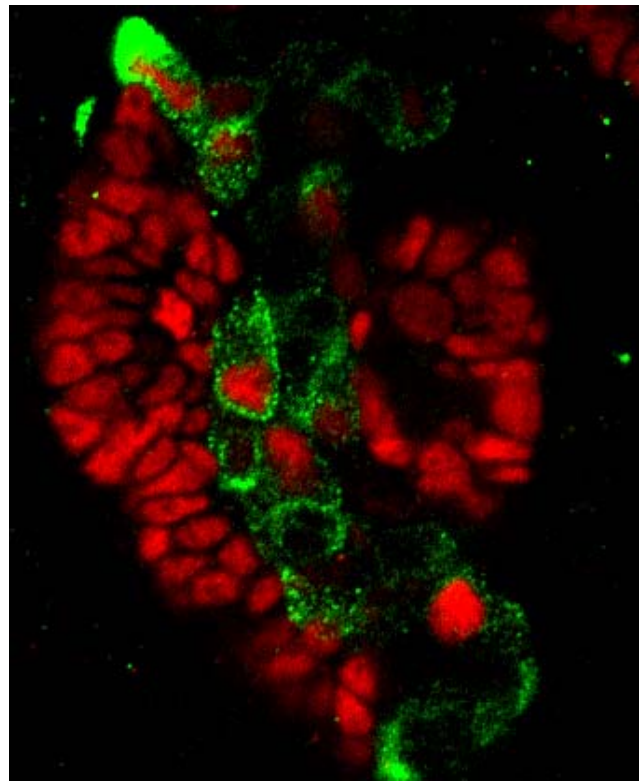


E12.5 Pdx1 Caspase-3

# In vitro proliferation

C

D
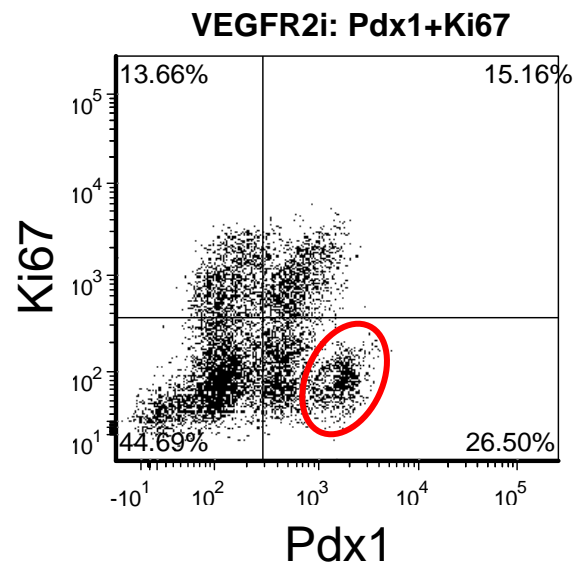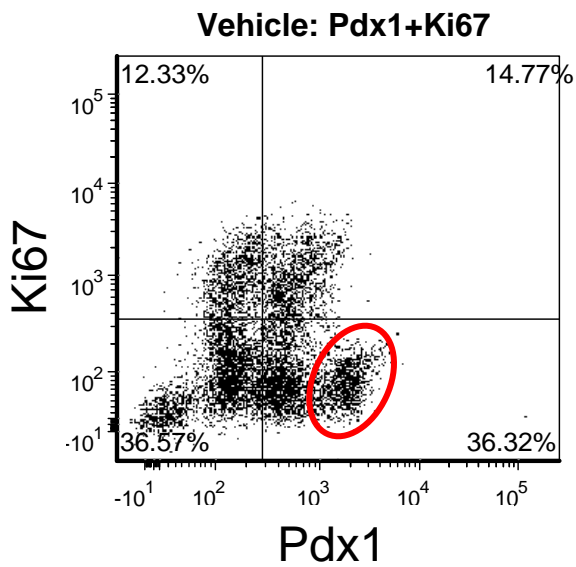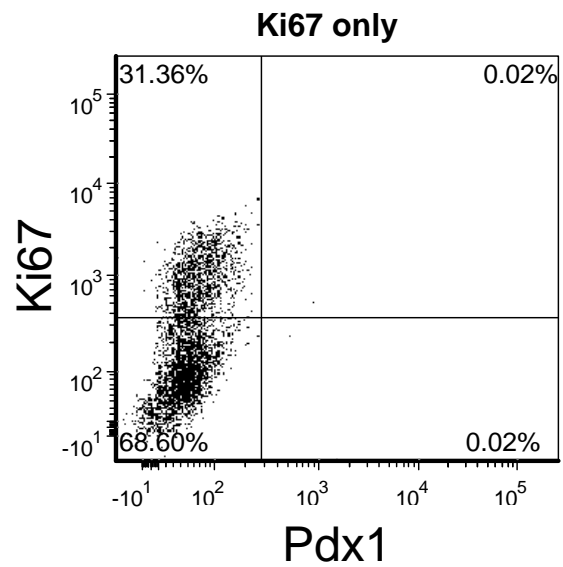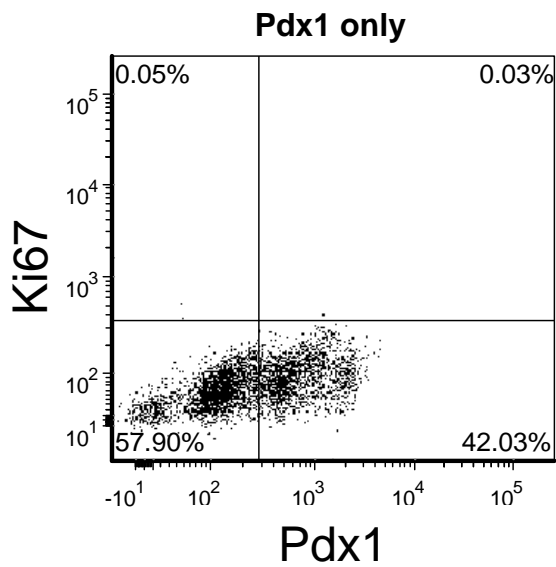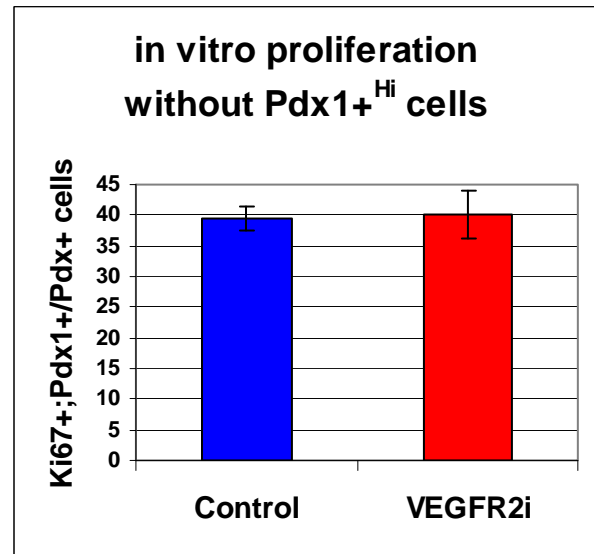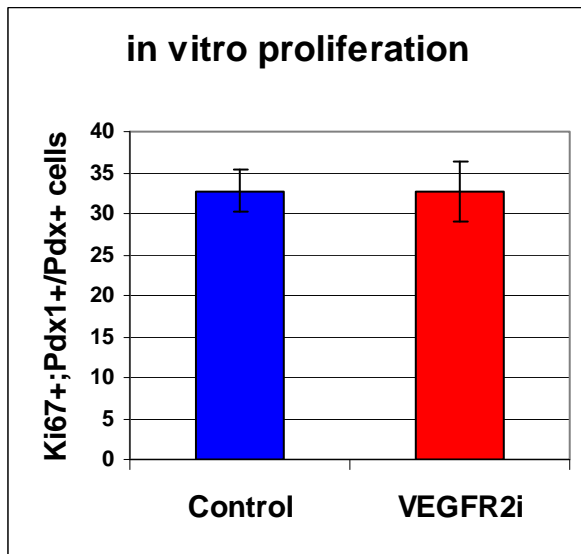
In vitro Apoptosis
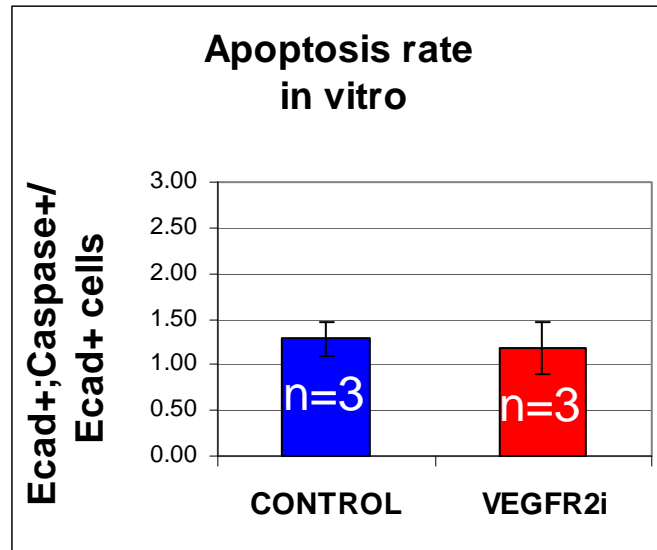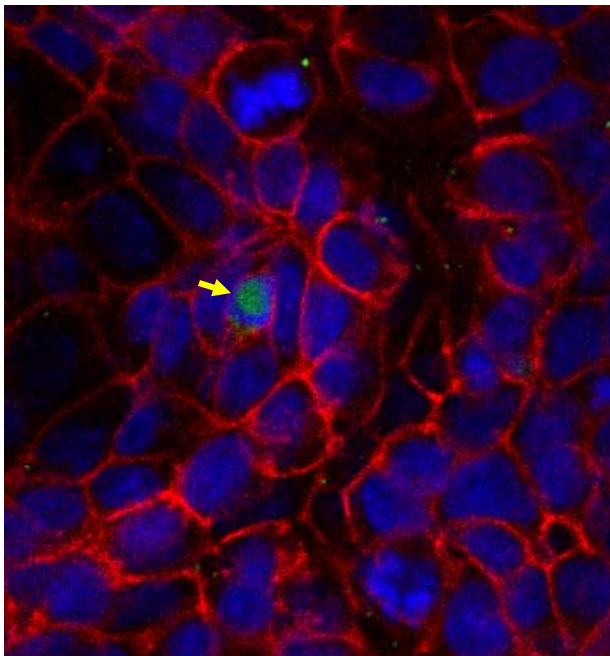


Control            VEGFR2i
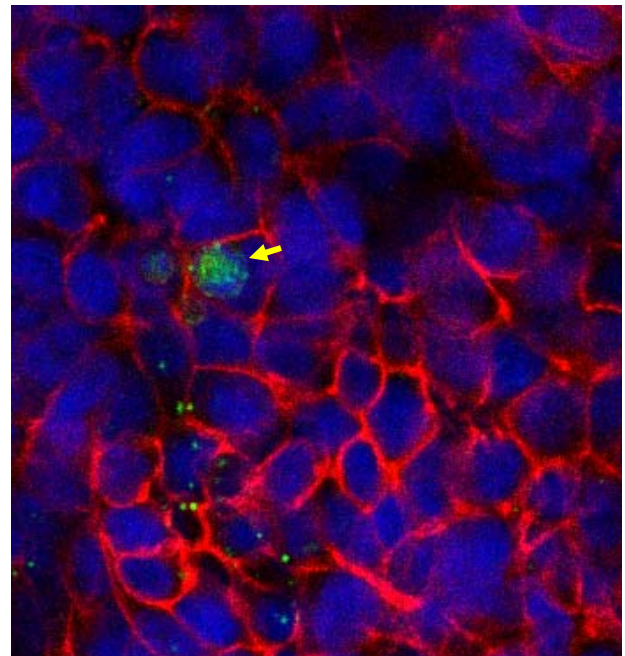
E-cad Caspase-3 Nuclei

E-cad



**Control**

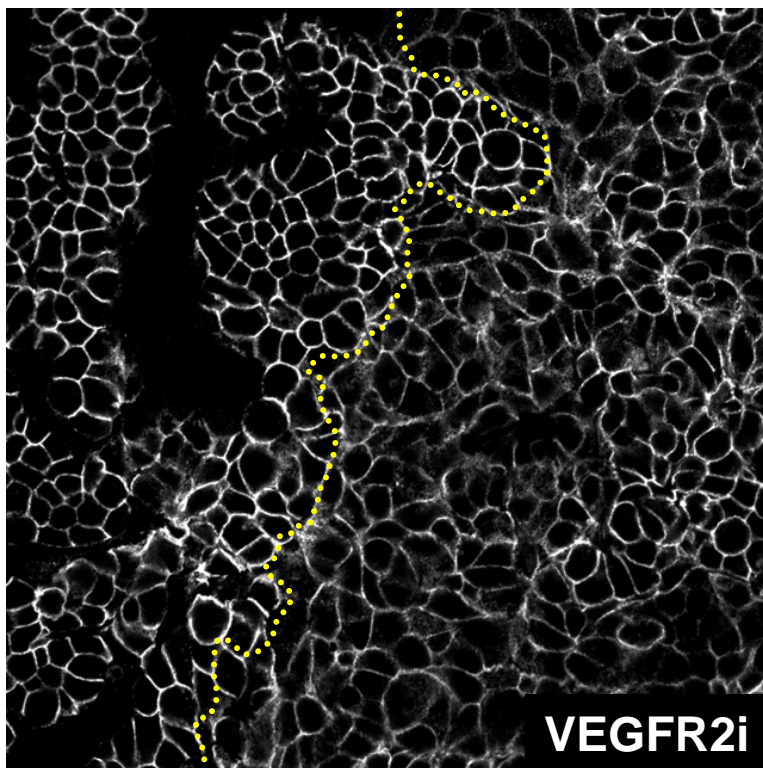E-cad



**VEGFR2i**
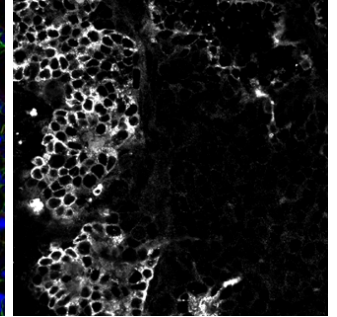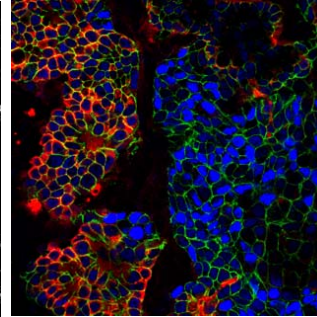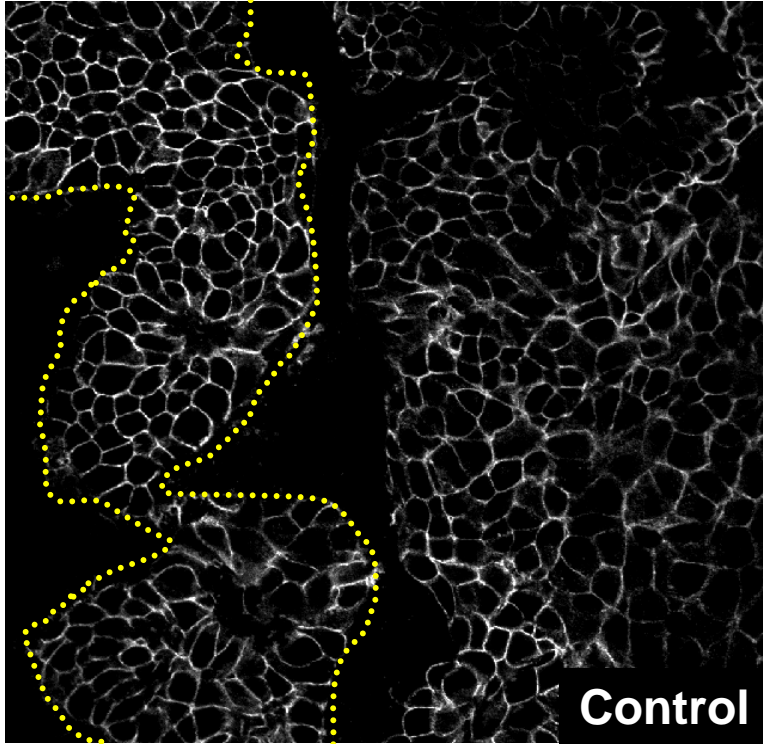
**Amylase**
**E-cad**
**Pdx1**

Amylase



**Cell size (E-cad boundary)**

**Area in pixels**
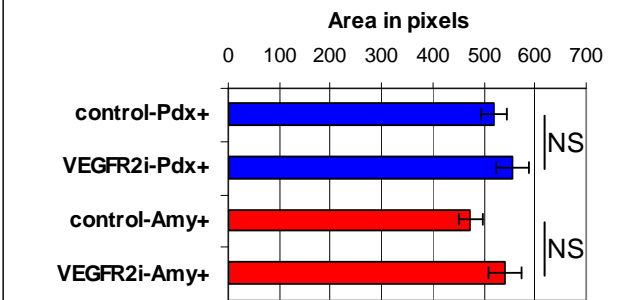


**Amylase**
**E-cad**
**Pdx1**

Amylase

**Table S1. Transcriptome changes following overexpression of VEGF in vivo: upregulated genes**

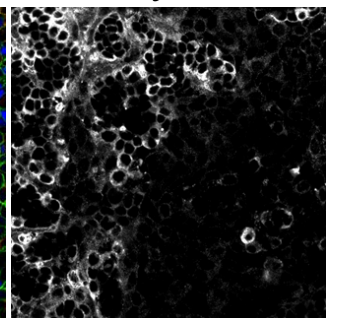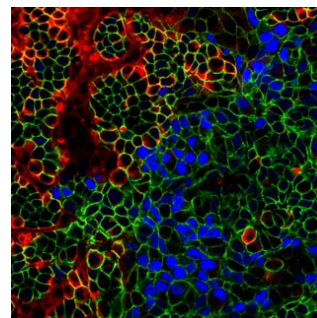| | Gene | Gene_assignment.2 | *P*-value | Fold |
|---|---|---|---|---|
| 1 | *Ppbp* | Pro-platelet basic protein | 0.00749356 | 5.53 |
| 2 | *Alb* | Albumin (Alb), mRNA | 0.00142908 | 5.16 |
| 3 | *Esm1* | Endothelial cell-specific molecule 1 | 0.00282063 | 3.37 |
| 4 | *Hbb-bh1* | Hemoglobin Z, beta-like embryonic chain | 0.000106173 | 3.29 |
| 5 | *Car2* | Carbonic anhydrase 2 | 0.0166405 | 2.59 |
| 6 | *Slc4a1* | Solute carrier family 4 (anion exchanger), member 1 | 0.00102512 | 2.58 |
| 7 | *Oit3* | Oncoprotein induced transcript 3 | 0.00196738 | 2.55 |
| 8 | *Lhx9* | LIM homeobox protein 9 | 0.00879942 | 2.27 |
| 9 | *Rhag* | Rhesus blood group-associated A glycoprotein | 0.00188723 | 2.19 |
| 10 | *Kel* | Kell blood group (Kel), mRNA | 0.0106346 | 2.04 |
| 11 | *Cd34* | CD34 antigen | 0.00155023 | 2.03 |
| 12 | *Alas2* | Aminolevulinic acid synthase 2, erythroid | 0.000380454 | 2.02 |
| 13 | *Gpm6a* | Glycoprotein m6a | 0.000873065 | 1.93 |
| 14 | *Irak1bp1* | Interleukin-1 receptor-associated kinase 1 binding prot | 0.0700767 | 1.92 |
| 15 | *Hsd3b6* | Hydroxy-delta-5-steroid dehydrogenase, 3 beta- and steroi | 0.00277503 | 1.91 |
| 16 | *Hba-x* | Hemoglobin X, alpha-like embryonic chain in Hba c | 0.000701182 | 1.90 |
| 17 | *Tnc* | Tenascin C | 0.0237128 | 1.90 |
| 18 | *Flt4* | FMS-like tyrosine kinase 4 | 0.0117201 | 1.89 |
| 19 | *9430028L06Rik* | RIKEN cDNA 9430028L06 gene | 0.000281261 | 1.86 |
| 20 | *Flt1* | FMS-like tyrosine kinase 1 | 0.000148862 | 1.86 |
| 21 | *Ehd3* | EH-domain containing 3 | 0.0228445 | 1.85 |
| 22 | *Tm4sf5* | Transmembrane 4 superfamily member 5 | 0.0236431 | 1.84 |
| 23 | *Gypa* | Glycophorin A | 0.0659538 | 1.83 |
| 24 | *Itgb3* | Integrin beta 3 (Itgb3), mRNA | 0.00145498 | 1.82 |
| 25 | *Klhl6* | Kelch-like 6 (Drosophila) (Klhl6), mRNA | 0.0253863 | 1.82 |
| 26 | *Pdgfb* | Platelet derived growth factor, B polypeptide | 0.0101908 | 1.82 |
| 27 | *Upk1b* | Uroplakin 1B (Upk1b), mRNA | 0.00531255 | 1.81 |
| 28 | *Rspo3* | R-spondin 3 homolog (Xenopus laevis) | 0.0265898 | 1.81 |
| 29 | *Pim1* | Proviral integration site 1 | 0.00390876 | 1.80 |
| 30 | *Bmp4* | Bone morphogenetic protein 4 | 0.0196398 | 1.80 |

**Table S2. Transcriptome changes following overexpression of VEGF in vivo: downregulated genes**

| | Gene | Gene_assignment.2 | *P*-value | Fold |
|---|---|---|---|---|
| 1 | *Neurog3* | Neurogenin 3 | 0.00540351 | 0.16 |
| 2 | *Pcsk2* | Proprotein convertase subtilisin/kexin type 2 | 0.000814316 | 0.17 |
| 3 | *Tmem27* | Transmembrane protein 27 | 0.000799818 | 0.22 |
| 4 | *Ctrb1* | Chymotrypsinogen B1 | 0.000230162 | 0.24 |
| 5 | *Clps* | Colipase, pancreatic | 0.00233391 | 0.27 |
| 6 | *Scg3* | Secretogranin III | 0.00481541 | 0.28 |
| 7 | *Rfxdc1* | Regulatory factor X domain containing 1 | 0.000178519 | 0.29 |
| 8 | *Chga* | Chromogranin A | 0.000430345 | 0.30 |
| 9 | *Pnliprp1* | Pancreatic lipase related protein 1 | 0.00126757 | 0.30 |
| 10 | *Chgb* | Chromogranin B | 0.00426781 | 0.32 |
| 11 | *Slc38a5* | Solute carrier family 38, member 5 | 0.000806704 | 0.32 |
| 12 | *Cck* | Cholecystokinin | 0.00090555 | 0.32 |
| 13 | *Neurod1* | Neurogenic differentiation 1 | 0.000731695 | 0.33 |
| 14 | *Ptprn2* | Protein tyrosine phosphatase, receptor type, N polypeptid | 0.00053729 | 0.34 |
| 15 | *Pyy* | Peptide YY | 0.00128277 | 0.35 |
| 16 | *Pou3f4* | POU domain, class 3, transcription factor 4 (BRN4) | 0.0108799 | 0.35 |
| 17 | *Kcnk16* | Potassium channel, subfamily K, member 16 | 0.000533469 | 0.37 |
| 18 | *Cpa2* | Carboxypeptidase A2, pancreatic | 0.00282555 | 0.38 |
| 19 | *Gcg* | Glucagon | 0.000367909 | 0.39 |
| 20 | *Abcc8* | ATP-binding cassette, sub-family C (CFTR/MRP), member 8 | 0.00085962 | 0.40 |
| 21 | *Pax6* | Paired box gene 6 | 0.0206573 | 0.41 |
| 22 | *Rbp4* | Retinol binding protein 4, plasma (Rbp4), mRNA | 0.00508347 | 0.43 |
| 23 | *Tmem171* | Transmembrane protein 171 | 0.00678058 | 0.43 |
| 24 | *Nkx2-2* | NK2 transcription factor related, locus 2 (Drosophila) | 0.00647539 | 0.45 |
| 25 | *Lgals3bp* | Lectin, galactoside-binding, soluble, 3 binding protein | 0.0259632 | 0.45 |
| 26 | *Ttr* | Transthyretin | 0.000346445 | 0.45 |
| 27 | *Dub2a* | Deubiquitinating enzyme 2a | 0.00905913 | 0.47 |
| 28 | *Gpr119* | G-protein coupled receptor 119 | 0.00454876 | 0.47 |
| 29 | *Cpb2* | Carboxypeptidase B2 (plasma) | 0.00059552 | 0.47 |
| 30 | *Nudt11* | Nudix (nucleoside diphosphate linked moiety X) | 0.0339547 | 0.48 |

**Table S3. Transcriptome changes following vascular ablation ex vivo: upregulated genes**

| | Gene | Gene_assignment.2 | *P*-value | Fold |
|---|---|---|---|---|
| 1 | *EG436523* | Predicted gene, EG436523 | 0.00853873 | 3.72 |
| 2 | *2210010C04Rik* | RIKEN cDNA 2210010C04 gene | 0.0019915 | 2.92 |
| 3 | *Sycn* | Syncollin (Sycn), mRNA | 0.000821856 | 2.80 |
| 4 | *Cpb1* | Carboxypeptidase B1 (tissue) | 2.98E-06 | 2.61 |
| 5 | *Rnase1* | Ribonuclease, RNase A family, 1 (pancreatic) | 0.00342149 | 2.49 |
| 6 | *Ela3* | Elastase 3, pancreatic | 0.0226504 | 2.33 |
| 7 | *Try10* | Trypsin 10 | 0.000243102 | 2.32 |
| 8 | *Sostdc1* | Sclerostin domain containing 1 | 0.000358236 | 2.16 |
| 9 | *Reg1* | Regenerating islet-derived 1 | 0.000813943 | 2.15 |
| 10 | *Pdia2* | Protein disulfide isomerase associated 2 | 0.00538114 | 2.13 |
| 11 | *Arhgdig* | Rho GDP dissociation inhibitor (GDI) gamma | 0.00327278 | 1.95 |
| 12 | *Spink3* | Serine peptidase inhibitor, Kazal type 3 | 0.0354314 | 1.95 |
| 13 | *EG386551* | Predicted gene, EG386551 | 0.0037101 | 1.93 |
| 14 | *Bhlhb8* | Basic helix-loop-helix domain containing, class B, 8 | 0.00399569 | 1.93 |
| 15 | *1810009J06Rik* | RIKEN cDNA 1810009J06 gene | 0.0136482 | 1.91 |
| 16 | *Clps* | Colipase, pancreatic | 0.00057275 | 1.88 |
| 17 | *Aldh1a1* | Aldehyde dehydrogenase family 1, subfamily A1 | 0.000312059 | 1.87 |
| 18 | *Sprr1a* | Small proline-rich protein 1A | 0.0352784 | 1.86 |
| 19 | *Prss3* | Protease, serine, 3 | 0.00996311 | 1.85 |
| 20 | *RP23-395H4.4* | Elastase 2A | 0.00391122 | 1.84 |
| 21 | *LOC667824* | Similar to Glutathione S-transferase Mu 3 (GST class-m | 0.0215044 | 1.77 |
| 22 | *Ugt2b34* | UDP glucuronosyltransferase 2 family, polypeptide B34 | 0.00121451 | 1.77 |
| 23 | *Nov* | Nephroblastoma overexpressed gene | 0.00452824 | 1.77 |
| 24 | *F10* | Coagulation factor X | 0.00999271 | 1.77 |
| 25 | *Edaradd* | EDAR (ectodysplasin-A receptor)-associated death domain | 0.0146405 | 1.77 |
| 26 | *Mat1a* | Methionine adenosyltransferase I, alpha | 0.00855411 | 1.76 |
| 27 | *Tc2n* | Tandem C2 domains, nuclear | 0.0591035 | 1.75 |
| 28 | *Gstm1* | Glutathione S-transferase, mu 1 | 0.00802741 | 1.73 |
| 29 | *1810009J06Rik* | RIKEN cDNA 1810009J06 gene | 0.0314361 | 1.73 |
| 30 | *Prss3* | Protease, serine, 3 | 0.000982799 | 1.71 |

**Table S4. Transcriptome changes following vascular ablation ex vivo: downregulated genes**

| | Gene | Gene_assignment.2 | *P*-value | Fold |
|---|---|---|---|---|
| 1 | *Prnd* | Prion protein dublet (Prnd), mRNA | 0.000189119 | 0.05 |
| 2 | *Cdh5* | Cadherin 5 (Cdh5), mRNA | 0.00160228 | 0.06 |
| 3 | *Cd93* | CD93 antigen | 0.000675474 | 0.06 |
| 4 | *Pecam1* | Platelet/endothelial cell adhesion molecule 1 | 0.00177616 | 0.10 |
| 5 | *Esm1* | Endothelial cell-specific molecule 1 | 0.000714103 | 0.11 |
| 6 | *Emcn* | Endomucin (Emcn), mRNA | 0.00348785 | 0.11 |
| 7 | *Gja5* | Gap junction membrane channel protein alpha 5 | 0.00246124 | 0.12 |
| 8 | *Tie1* | Tyrosine kinase receptor 1 (Tie1), mRNA | 0.00162247 | 0.12 |
| 9 | *Gpr116* | G protein-coupled receptor 116 | 0.000566763 | 0.15 |
| 10 | *Bcl6b* | B-cell CLL/lymphoma 6, member B | 0.00514539 | 0.15 |
| 11 | *Esam1* | Endothelial cell-specific adhesion molecule | 0.0090255 | 0.16 |
| 12 | *Mmrn2* | Multimerin 2 | 0.00189719 | 0.17 |
| 13 | *Cxcr4* | Chemokine (C-X-C motif) receptor 4 | 0.000659435 | 0.17 |
| 14 | *Gja4* | Gap junction protein, alpha 4 | 0.00312086 | 0.18 |
| 15 | *Rasip1* | Ras interacting protein 1 | 0.00496424 | 0.19 |
| 16 | *Flt1* | FMS-like tyrosine kinase 1 | 0.00303612 | 0.20 |
| 17 | *Hbb-y* | Hemoglobin Y, beta-like embryonic chain | 0.000208694 | 0.21 |
| 18 | *Gimap4* | GTPase, IMAP family member 4 | 0.0449576 | 0.22 |
| 19 | *Cldn5* | Claudin 5 | 0.0112778 | 0.22 |
| 20 | *Gimap6* | GTPase, IMAP family member 6 | 5.84E-05 | 0.23 |
| 21 | *Kdr* | Kinase insert domain protein receptor | 0.00152495 | 0.23 |
| 22 | *Sox7* | SRY-box containing gene 7 | 0.00602817 | 0.24 |
| 23 | *Edg1* | Endothelial differentiation sphingolipid G-protein | 0.00211202 | 0.25 |
| 24 | *6430550H21Rik* | RIKEN cDNA 6430550H21 gene | 0.00145396 | 0.27 |
| 25 | *Clec14a* | C-type lectin domain family 14, member a | 0.00560583 | 0.29 |
| 26 | *Fxyd5* | FXYD domain-containing ion transport regulator 5 | 0.000454525 | 0.29 |
| 27 | *Ebf1* | Early B-cell factor 1 | 0.00328631 | 0.30 |
| 28 | *Erg* | Avian erythroblastosis virus E-26 (v-ets) oncogene related / | 0.000896231 | 0.30 |
| 29 | *Epas1* | Endothelial PAS domain protein 1 | 0.00213816 | 0.30 |
| 30 | *Fli1* | Friend leukemia integration 1 | 0.000542625 | 0.30 |